Stem Cell Reports
Article
OPEN ACCESS

Enhanced Hematopoietic Stem Cell Function Mediates Immune Regeneration following Sex Steroid Blockade

Danika M. Khong,[1,3,5] Jarrod A. Dudakov,[1,2,3,*] Maree V. Hammett,[1] Marc I. Jurblum,[1] Sacha M.L. Khong,[1,6] Gabrielle L. Goldberg,[1] Tomoo Ueno,[1] Lisa Spyroglou,[1] Lauren F. Young,[1] Marcel R.M. van den Brink,[2] Richard L. Boyd,[1,4] and Ann P. Chidgey[1,4,*]

[1]Stem Cells and Immune Regeneration Laboratory, Department of Anatomy and Developmental Biology, Monash University, Clayton, VIC 3800, Australia
[2]Immunology Program, Memorial Sloan-Kettering Cancer Center, New York, NY 10065, USA
[3]Co-first author
[4]Co-senior author
[5]Present address: Massachusetts General Hospital, Harvard Medical School, Harvard University, Boston, MA 02114, USA
[6]Present address: Department of Surgery, Stanford University, Stanford, CA 94305, USA
*Correspondence: dudakovj@mskcc.org (J.A.D.), ann.chidgey@monash.edu (A.P.C.)
http://dx.doi.org/10.1016/j.stemcr.2015.01.018

SUMMARY

Mechanisms underlying age-related defects within lymphoid-lineages remain poorly understood. We previously reported that sex steroid ablation (SSA) induced lymphoid rejuvenation and enhanced recovery from hematopoietic stem cell (HSC) transplantation (HSCT). We herein show that, mechanistically, SSA induces hematopoietic and lymphoid recovery by functionally enhancing both HSC self-renewal and propensity for lymphoid differentiation through intrinsic molecular changes. Our transcriptome analysis revealed further hematopoietic support through rejuvenation of the bone marrow (BM) microenvironment, with upregulation of key hematopoietic factors and master regulatory factors associated with aging such as Foxo1. These studies provide important cellular and molecular insights into understanding how SSA-induced regeneration of the hematopoietic compartment can underpin recovery of the immune system following damaging cytoablative treatments. These findings support a short-term strategy for clinical use of SSA to enhance the production of lymphoid cells and HSC engraftment, leading to improved outcomes in adult patients undergoing HSCT and immune depletion in general.

INTRODUCTION

One key etiological factor underlying a wide range of diseases is the progressive decline in immune function with age (Dorshkind et al., 2009). At its core is a reduction in lymphopoiesis within the bone marrow (BM) and thymus (Miller and Allman, 2003; Rodewald, 1998), attributed in part to a decrease in the number and function of lymphoid progenitors (Min et al., 2004, 2006). Increasing evidence suggests that intrinsic changes to the earliest hematopoietic stem cells (HSCs) also contribute toward age-related immune degeneration (Geiger et al., 2013). Deficiency in DNA repair, altered DNA methylation patterns, aberrant metabolism and reactive oxygen species, and skewed upregulation of myeloid- (at the expense of lymphoid-) associated genes all contribute to altered HSC function with age (expertly reviewed in Geiger et al., 2013). However, in addition to intrinsic functional changes, extrinsic alterations to the HSC niche also likely to contribute toward the degeneration of HSC function with age (Woolthuis et al., 2011).

Evidence suggests that sex steroids play at least some role in age-related degeneration of lymphopoiesis (Chinn et al., 2012), and we, and others, have previously shown that sex steroid ablation (SSA) is able to rejuvenate aged and immunodepleted BM and thymus, enhance peripheral T and B cell function, and promote immune recovery following hematopoietic stem cell transplantation (HSCT) (Dudakov et al., 2009a; Goldberg et al., 2009; Heng et al., 2005; Sutherland et al., 2005; Velardi et al., 2014). However, the mechanisms underlying SSA-mediated immune regeneration are still unresolved. In particular, the effects of SSA on hematopoietic stem and progenitor cells (HSPCs) are likely to be pertinent given that sex steroids regulate HSC function as well as lymphoid-primed multipotent progenitor (LMPP) cells (Medina et al., 2001; Nakada et al., 2014; Thurmond et al., 2000). In this study, we sought to examine the events upstream of SSA-mediated lymphoid regeneration, focusing on the earliest HSPCs.

RESULTS

SSA Increases the Number of Hematopoietic Stem and Progenitor Cells

Although age-induced reduction in HSC function does not reach its nadir until at least 24 months of age in mice (Morrison et al., 1996), it is clear that significant defects in the capacity for T and B cell differentiation are already evident by middle age (9 months) (Dudakov et al., 2009a; Heng et al., 2005; Sutherland et al., 2005). To determine whether

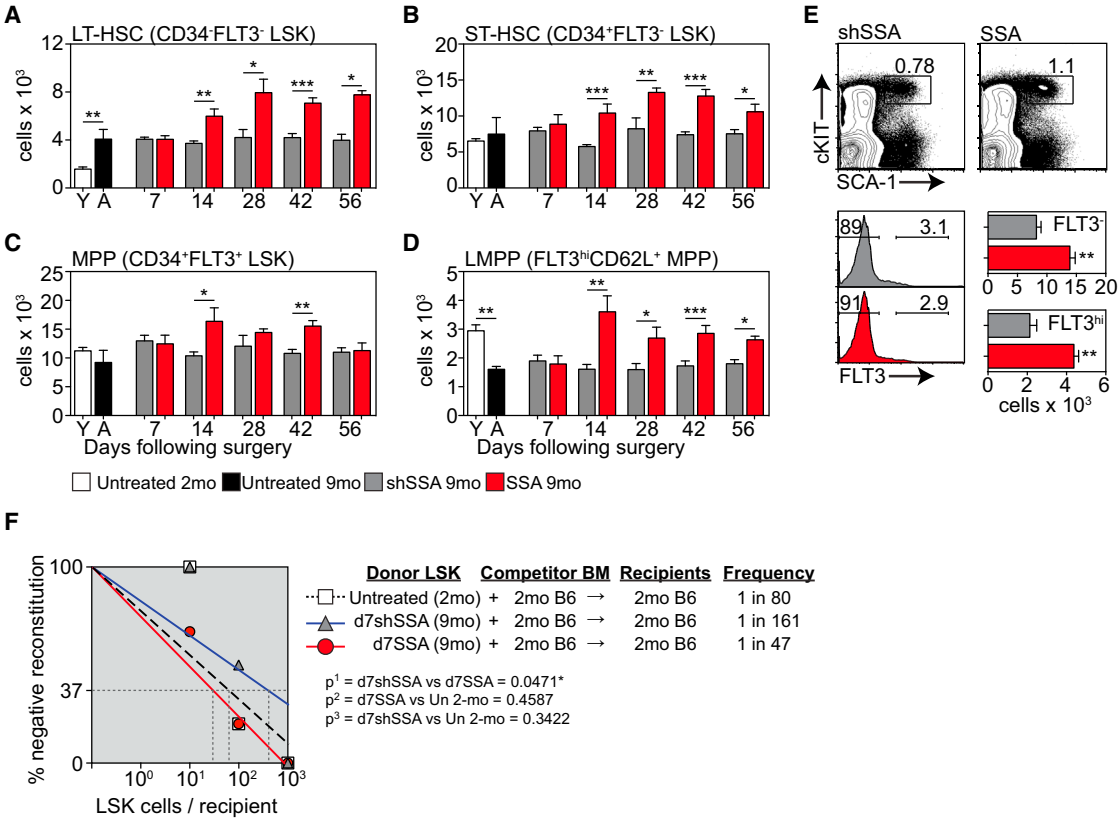

Figure 1. SSA Increases the Number of Multilineage HSCs in Middle-Aged Mice

(A–D) Lin$^-$SCA1$^+$cKIT$^+$ (LSK) BM can be subdivided into populations of LT-HSCs (CD34$^-$FLT3$^-$), ST-HSCs (CD34$^+$FLT3$^-$), and MPPs (CD34$^+$FLT3$^+$). The MPP population can be further fractionated based on FLT3 and CD62L expression for analysis of LMPPs (FLT3^{hi}CD62L$^+$). Absolute number of LT-HSCs (A), ST-HSCs (B), MPPs (C), and LMPPs (D) (n = 5–12/group/time point).

(E) Concatenated flow cytometry plots, gated on Lineage$^-$ cells, and absolute number of FLT3$^-$ LSK cells, 1 year after surgical SSA of 9-month male mice (n = 5/group).

(F) LSK cells were FACS purified from untreated CD45.2$^+$ 2-month; CD45.2$^+$ 9-month mice 7 days following surgical shSSA (d7shSSA); or CD45.2$^+$ 9-month mice 7 days following surgical SSA (d7SSA) (n = 6 recipients/group/dose) and graded doses of cells were transferred into lethally irradiated congenic CD45.1 recipients along with 5 × 10^5 CD45.1$^+$ supporting BM cells. Multilineage reconstitution (>1% B cell, T cell, macrophage, and granulocyte) was analyzed 12 weeks after transplant and the frequency of repopulating cells was calculated by Poisson statistics.

Bar graphs represent mean ± SEM. *p < 0.05, **p < 0.01, ***p < 0.001. See also Figures S1 and S2.

SSA initiates its impact early in hematopoiesis, we enumerated HSCs by flow cytometry (Figure S1A) at multiple time points after surgical castration of 9-month-old mice. Consistent with previous reports, there was a phenotypic increase in the absolute number of long-term HSCs (LT-HSCs) during aging with a 2-fold increase by middle age (Figure 1A). Following SSA, there was a further increase in the absolute number of LT-HSCs and short-term HSCs (ST-HSCs) from day 14 (d14SSA), which was maintained through to d56SSA compared to sham-SSA (shSSA) control mice (Figures 1A and 1B). While there was no observable impact of age on multipotent progenitors (MPPs), and SSA did not significantly alter their total number (Figure 1C), there was a selective decrease in LMPPs by 9 months, which was reversed following SSA (Figure 1D). This change in HSC number caused by SSA was extremely long-lived with increases in FLT3$^-$ (LT-HSC and ST-HSC) and FLT3^{hi} (LMPPs) still observed 1 year later (Figure 1E).

A defining characteristic of HSC function is the ability to differentiate into multiple lineages. The frequency of multilineage repopulating cells was therefore enumerated using a limiting-dilution competitive repopulation assay (Figure 1F). 10, 100, or 1,000 fluorescence-activated-cell-sorted (FACS) lineage-negative, Sca1$^+$, c-Kit$^+$ (LSK) cells from untreated 2-month mice; 9-month mice 7 days following sham surgery (9-month d7shSSA); or 9-month mice 7 days following surgical SSA (9-month d7SSA) were transferred along with 5 × 10^5 supporting BM cells into

lethally irradiated congenic recipients. We chose the d7SSA time point to better delineate qualitative from quantitative changes in HSCs as this was prior to any SSA-induced increase in absolute cell number (Figure 1A). Given there was no quantitative or functional differences in HSCs between untreated 9-month and 9-month shSSA mice (Figures 1A and S1B), all of our functional studies compared SSA mice to age-matched shSSA and untreated 2-month mice. Mice were considered reconstituted by a single HSC if there was $\geq$1% contribution of donor cells within both lymphoid (T and B cells) and myeloid (macrophage and granulocyte) lineages 12 weeks after transplant (Figure 1F). While there was no decrease in the frequency of multilineage repopulating cells in 9-month d7shSSA compared to 2-month mice (Figure 1F), functional LSK cells from 9-month d7SSA were significantly increased compared to 9-month d7shSSA controls (Figure 1F). When individual lineages were analyzed, mice reconstituted with 9-month d7SSA LSKs had an increased frequency of B-lineage and macrophage reconstituting cells (Figure S1C). All recipients, regardless of the number of cells transplanted, had detectable levels of granulocyte engraftment (data not shown), and there were no significant differences detected in T cell engraftment (Figure S1C). Ki67 and Annexin V (AnnV) were used to determine whether the increase in functional HSC frequency was due to a change in their cycling status or apoptosis. At day 7, there was no change in Ki67 or AnnV expression on $CD34^-$, $CD34^+$, or $CD34^+CD62L^+$ LSK subsets following SSA (Figures S1D and S1E).

SSA Significantly Enhances HSC Repopulation Potential

To assess long-term functional capacity for multilineage reconstitution, BM (2.5×10^6 cells) from 9-month $CD45.1^+$ d7shSSA or d7SSA was co-transplanted at a 1:1 ratio with congenic untreated young (2 month) competitor BM into lethally irradiated 2-month $CD45.2^+$ recipients. Over the 17 weeks analyzed, total $CD45.1^+$ donor-derived peripheral leukocyte reconstitution of mice transplanted with 9-month d7SSA BM was significantly higher than those reconstituted by 9-month d7shSSA mice (Figures 2A and 2B). Reflecting this, 9-month d7SSA-derived BM significantly improved B cell engraftment, while T cell engraftment transiently increased at 4 weeks after transplant compared to 9-month d7shSSA controls (Figure 2C). However, enhanced reconstitution by d7SSA was not restricted to the lymphoid compartment, with a significant improvement also observed in engraftment of both monocytes/macrophages and granulocytes (Figure 2C).

To determine the intrinsic impact on the stem and progenitor cell compartment, 2,000 purified LSK cells from untreated 2-month, 9-month d7shSSA, or 9-month d7SSA mice were co-transplanted with 2×10^6 BM cells from untreated congenic competitors into lethally irradiated recipients. Although there was no age-induced impact at 9-month on the ability of donor cells to engraft the BM 28 days after transplant, 9-month d7SSA-LSK significantly increased the overall number of $CD45.1^+$ cells in the marrow (Figure 2D), comprising donor LSK cells as well as downstream $Lin^-SCA1^-cKIT^+$ myeloid and erythroid progenitors and $Lin^-IL7R\alpha^+cKIT^+$ CLP populations (Figure 2E). On the other hand, long-term peripheral repopulation was significantly impaired with 9-month d7shSSA compared to untreated 2-month LSK (Figures 2F and 2G). Over the same time frame, there was a significant increase in the repopulation potential of LSK cells isolated from 9-month d7SSA mice, restoring the reduced middle-aged (9 month) LSK repopulation potential to 2-month levels. Increased reconstitution consisted principally of improved B cells, but also improved long-term T cell repopulation at day 135 after transplant (Figure 2H). Although myeloid engraftment increased with age, primarily due to granulocyte engraftment (Figure 2H), we found that donor LSKs from 9-month d7SSA did not further increase this engraftment above that seen in recipients of 9-month shSSA LSK cells (Figure 2H).

Enhanced Repopulation Ability following SSA Is Not due to Improved Homing of HSCs

To assess whether improved homing of transplanted cells to the BM niche could explain our observed SSA-mediated improvements to HSC repopulation, we examined LSK cells for expression of the homing and adhesion molecules VLA-4, VLA-5, and CXCR4. Although we found a decrease in the proportion of LSK cells expressing VLA-4, VLA-5, and CXCR4 with age, there was no change in their expression following SSA (Figures S2A and S2B), suggesting that the impacts of SSA on HSCs were intrinsic to the cells' function. To directly examine the homing ability of LT-HSCs in vivo, we harvested BM from 9-month d7shSSA or d7SSA mice and transplanted into unablated congenic 2- or 9-month recipients at a saturating dose of 20×10^6 BM cell and homing and engraftment of donor LT-HSCs analyzed 40 hr later (Figure S2C). The same proportion of LT-HSCs homed to BM irrespective of the age of the recipient, the age of the donor, or whether donors had undergone SSA. This result also held true for downstream ST-HSCs and MPPs (data not shown). Consistent with previous studies (Dykstra et al., 2011; Liang et al., 2005), when the number of transfused LT-HSCs was taken into account, there was a significant decrease in HSC homing in recipients of 9-month shSSA and SSA BM, as well as in aged recipients in all groups (Figure S2D).

HSC Self-Renewal Is Improved following SSA

To assess the impact of SSA on HSC self-renewal, lethally irradiated 2-month CD45.2 mice were transplanted with

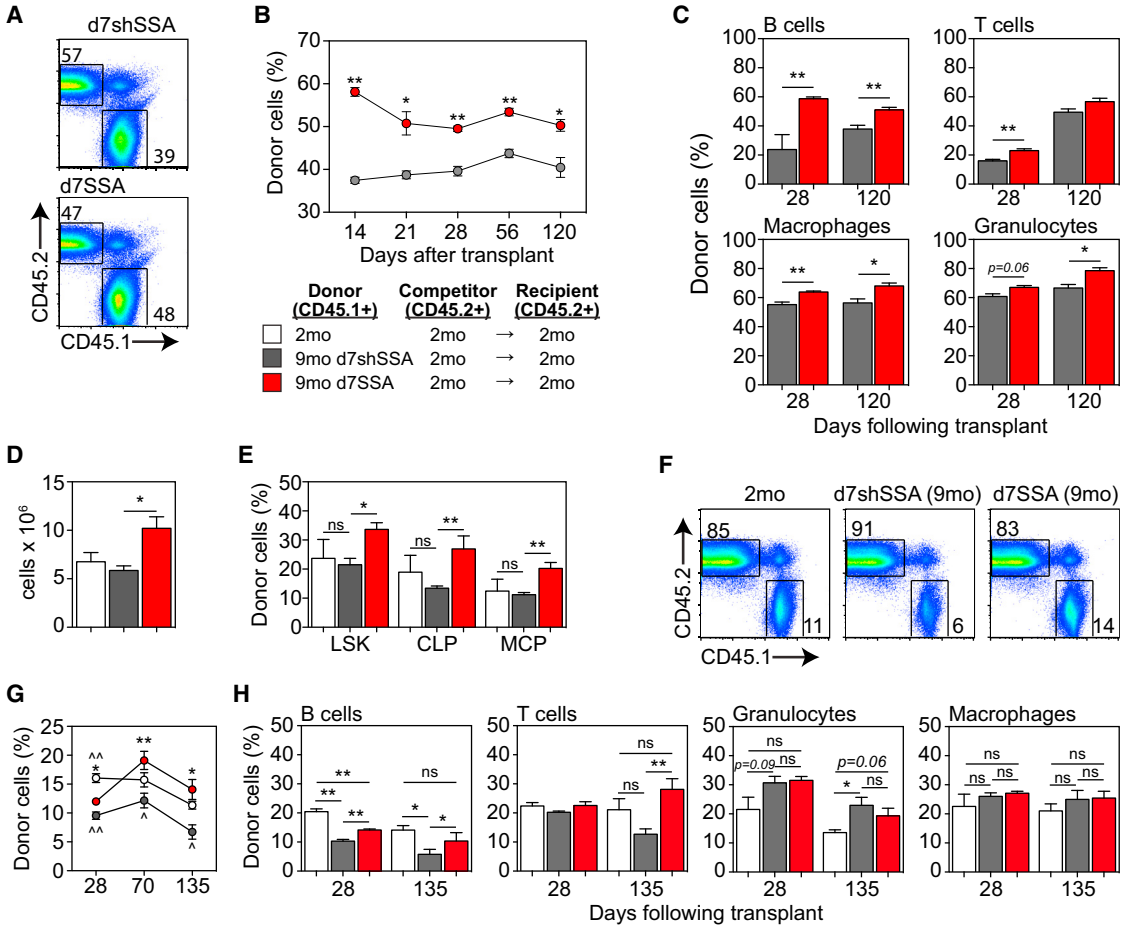

Figure 2. SSA Enhances the Functional Repopulation Potential of HSCs Derived from Middle-Aged Mice

(A–C) CD45.1 BM cells were harvested and pooled from 9-month d7shSSA, (n = 5 recipients/donor group) or 9-month d7SSA (n = 5 recipients/donor group) and 2.5 × 10^6 cells were transferred with an equal dose of untreated 2-month CD45.2 BM cells into lethally irradiated 2-month CD45.2 recipients. Reconstitution was analyzed at the designated time points. (A) Concatenated donor (CD45.1) versus competitor (CD45.2) flow cytometry profiles of spleen 17 weeks after transplant. (B) Total peripheral reconstitution measured by CD45.1 in spleen or peripheral blood over 120 days. (C) Lineage-specific reconstitution of $B220^+$ B cells, $TCR\beta^+$ T cells, $Gr1{+}CD11b^+$ granulocytes, and $Gr1^{lo}CD11b^+$ monocyte/macrophages in the spleen at 28 and 120 days after transplant.

(D–G) 2,000 FACS purified CD45.1 LSK cells from untreated 2-month; 9-month d7shSSA; or 9-month d7SSA were transferred along with 2 × 10^6 BM cells from untreated 2-month CD45.2 competitors into lethally irradiated CD45.2 recipients (n = 5–7/donor group). (D) Total number of CD45.1 donor-derived cells in the BM of recipients 28 days after transplant. (E) Proportion of $CD45.1^+$ whole BM, LSK, CLP, and MCP cells in the BM 28 days after transplant. (F) Concatenated donor (CD45.1) versus competitor (CD45.2) flow cytometry profiles of spleen 19 weeks after transplant. (G) Peripheral reconstitution in 28, 70, and 135 days after transplant. *Compared with 9-month shSS A mice. ^Compared with untreated 2-month mice.

(H) Lineage repopulation was measured among $B220^+$ B cells, $TCR\beta^+$ T cells, $Gr1^+CD11b^+$ granulocytes, and $Gr1^{lo}CD11b^+$ monocyte/macrophages.

Results are expressed as mean ± SEM. */^p < 0.05, **/^^p < 0.01, ***/^^^p < 0.001. See also Figure S2.

2,000 purified LSK cells from untreated 2-month, 9-month d7shSSA, or 9-month d7SSA mice together with 2.5 × 10^6 untreated congenic 2-month CD45.2 BM as support cells. 12 weeks after transplantation, 2.5 × 10^6 BM cells from primary recipients were transferred into secondary recipients along with 2.5 × 10^6 BM cells from untreated 2-month competitors. In both primary and secondary recipients, 9-month d7shSSA and untreated 2-month cells gave a similar level of donor engraftment, although with age there was a significant decline in the proportion of donor-derived cells upon secondary transplant (Figure 3A). However, 9-month d7SSA had significantly higher levels of engraftment in both primary and secondary recipients compared to cells from 9-month d7shSSA and untreated

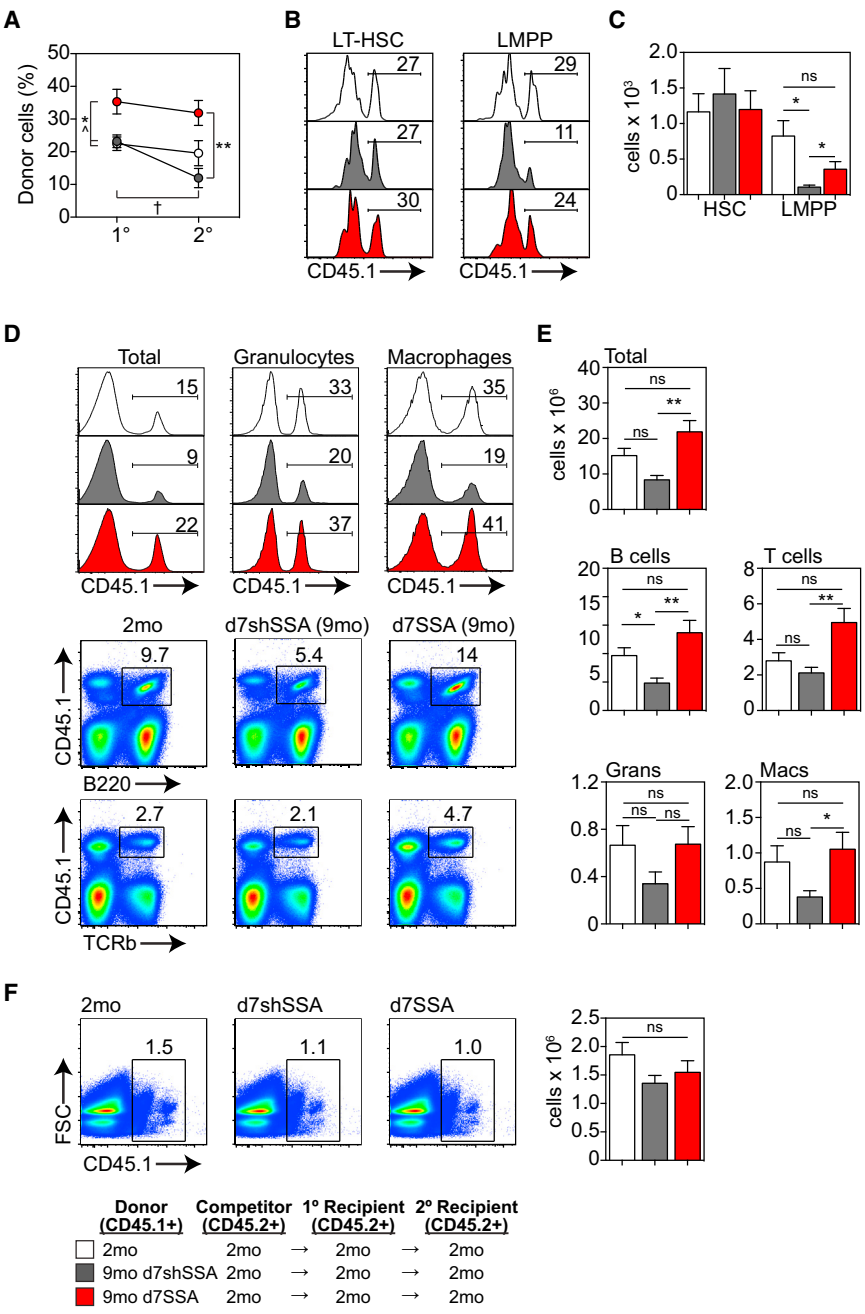

Figure 3. SSA Enhances the Self-Renewal Capacity of HSCs Derived from Middle-Aged Mice

2,000 CD45.1 purified LSK cells from CD45.1 2-month untreated, 9-month d7shSSA, or 9-month d7SSA were transferred along with 2.5 × 10^6 untreated 2-month CD45.2 BM cells into lethally irradiated 2-month CD45.2 primary recipients (n = 6 recipients/donor group, one individual recipient per individual donor). 12 weeks after transplant, primary recipient BM was harvested, and 2.5 × 10^6 BM cells were transplanted along with an equal dose of untreated 2-month CD45.2 BM cells into lethally irradiated 2-month CD45.2 secondary recipients (n = 12 recipient/donor groups, two recipients per individual donor). Reconstitution of secondary recipients was measured 12 weeks after transplant.

(A) Proportion of CD45.1$^+$ donor cells in BM 12 weeks following transplant in primary and secondary recipients (*Compared with 9-month d7shSSA mice within primary or secondary recipients. ^Compared to untreated 2-month mice within either primary or secondary recipients. †Compared to 9-month d7shSSA between primary and secondary recipients).

(B) Proportion of donor-derived CD150$^+$ CD34$^-$FLT3$^-$ LT-HSCs and CD34$^+$FLT3^{hi} CD62L$^+$ LMPPs in the BM of secondary recipients 12 weeks after transplant.

(C) Absolute number of donor-derived LT-HSCs and LMPPs in the BM of secondary recipients 12 weeks after transplant.

(D) Concatenated flow cytometric profiles of total donor reconstitution, as well as donor B220$^+$ B cells, TCRβ$^+$ T cells, Gr-1$^+$CD11b$^+$ granulocytes, and Gr1^{lo}CD11b$^+$ in the spleen of secondary recipients 12 weeks after transplant.

(E) Absolute number of CD45.1$^+$ donor cells in the spleen of secondary recipients 12 weeks after transplant.

(F) 12 weeks after secondary transplant, 2.5 × 10^6 BM cells from secondary recipients was transplanted into tertiary recipients at a 1:1 ratio with competitor CD45.2$^+$ BM, and peripheral reconstitution was assessed at 12 weeks. Concatenated FACS plots of the proportion, and the absolute number of CD45.1$^+$ donor cells, in tertiary recipients (n = 6/group).

Results are expressed as mean ± SEM. */^p < 0.05, **/^^p < 0.01.

2-month mice. Consistent with previous reports (Dykstra et al., 2011), there was a reduction in donor contribution between primary and secondary recipients when cells derived from 9-month d7shSSA mice were transplanted. In contrast, secondary recipients receiving 9-month d7SSA cells or 2-month cells showed no reduction in the proportion of total donor cells engrafted compared to the primary grafts (Figure 3A).

This defect in the reconstitution of secondary recipients was not attributable to a numerical reduction in stem cell

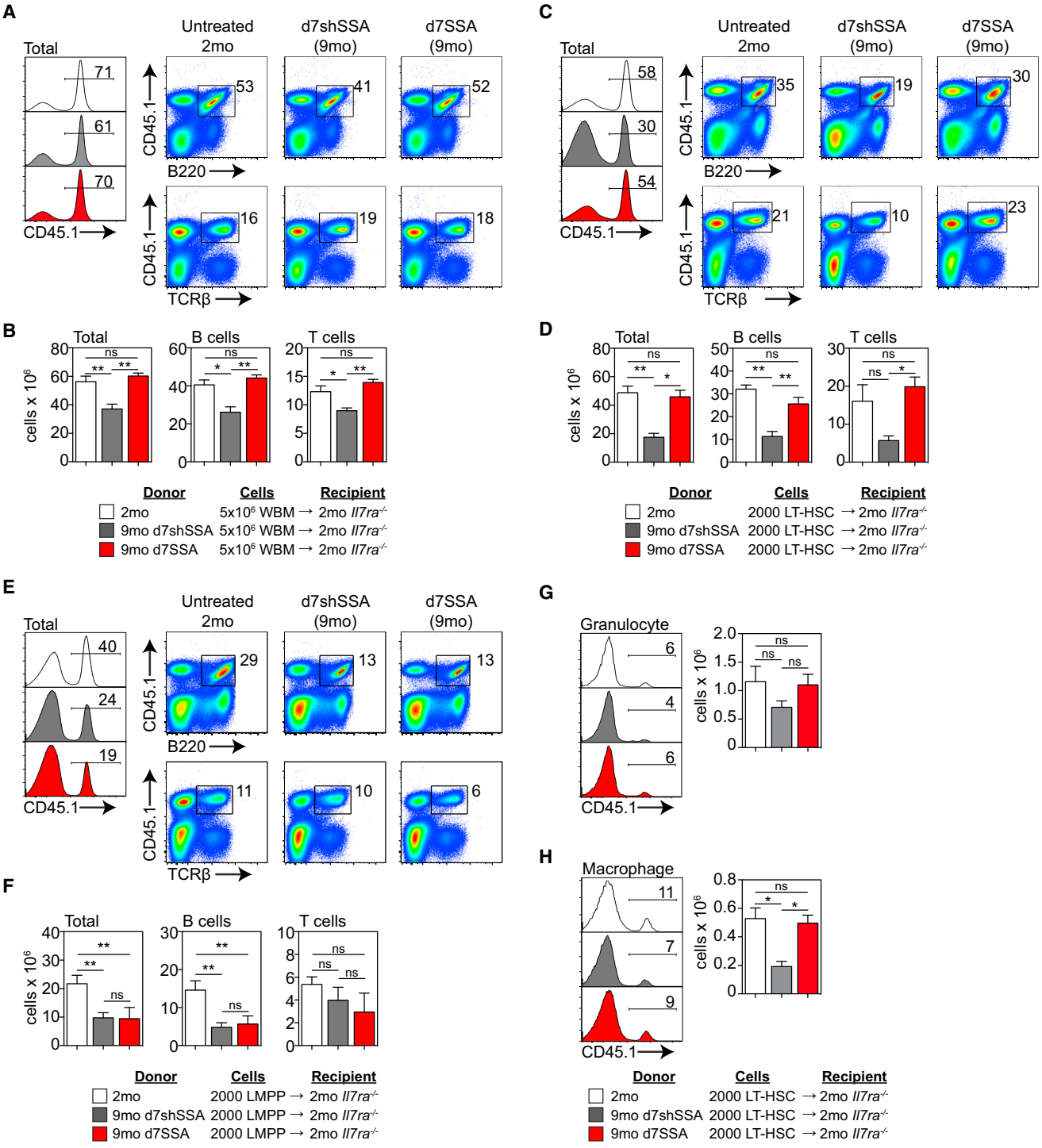

Figure 4. SSA Promotes Lymphoid Differentiation Potential of HSCs Derived from Middle-Aged Mice

(A and B) 5 × 10^6 CD45.1 BM cells from untreated 2-month; 9-month d7shSSA; or 9-month d7SSA were transferred into unablated 2-month *Il7ra*$^{-/-}$ recipients (n = 6 recipient/donor groups, one recipient per donor). (A) Concatenated flow cytometry plots displaying total donor reconstitution as well as donor Gr1^{+}CD11b^{+} granulocyte, Gr1^{lo}CD11b^{+} monocyte/macrophage, B220^{+} B cells, and TCRβ^{+} T cells reconstitution at day 42. (B) Absolute number of donor cells as well as the number of donor B cells and T cells at day 42.

(C and D, and G and H) 2,000 CD45.1 LT-HSCs from untreated 2-month; 9-month d7shSSA; or 9-month d7SSA were transferred into unablated 2-month *Il7ra*$^{-/-}$ recipients (n = 6 recipient/donor groups, one recipient per donor) and donor-derived hematopoiesis measured

(legend continued on next page)

engraftment, as there was no change in the proportion or number of donor-derived LT-HSCs in the BM of secondary recipients as a consequence of age or SSA (Figures 3B and 3C). However, consistent with the functional decline in lymphopoiesis with age, there was a significant decrease in donor-derived LMPPs from 9-month d7shSSA, which was reversed in secondary recipients of 9-month d7SSA cells (Figures 3B and 3C). Within specific hematopoietic lineages, although there was no loss in the proportion of donor-derived T cells or CD11b$^+$ myeloid cells with age, there was a decline in B cell reconstitution, which contributed toward a global decline in CD45$^+$ cells (Figures 3D and 3E). Importantly, secondary reconstitution from 9-month d7SSA BM significantly increased the donor contribution of all leukocyte subsets (Figures 3D and 3E), but this effect of SSA on HSC self-renewal was finite as there was no difference in donor contribution between 9-month d7shSSA and 9-month d7SSA in tertiary recipients (Figure 3F).

SSA Increased the Lymphoid Differentiation Capacity of LT-HSCs

The dominant downstream effects of SSA in steady-state aged mice are on lymphopoiesis, with little if any impact observed on myeloid cells. To test the lymphoid differentiation capacity of the BM as a whole, we transferred 5 × 10^6 BM cells derived from 2-month, 9-month d7shSSA, or 9-month d7SSA mice into unirradiated *Il7ra*$^{-/-}$ recipients, which bypasses the confounding effects of total body irradiation (TBI) (Gossens et al., 2009). We found a significant defect by 9 months in the ability of BM to engraft IL7Rα$^{-/-}$ recipients. As expected, this was predominantly composed of declines in donor-derived TCRβ$^+$ T cells and B220$^+$ B cells (Figures 4A and 4B). To test the relative functional changes between HSCs and their downstream progenitors, we transferred 2,000 LT-HSCs or LMPPs derived from untreated 2-month, 9-month d7shSSA, or 9-month d7SSA mice into unirradiated *Il7ra*$^{-/-}$ recipients. LT-HSCs isolated from 9-month d7shSSA mice exhibited reduced engraftment at day 70 compared to untreated 2-month LT-HSCs in both B and T cell lineages. However, *Il7ra*$^{-/-}$ recipients transplanted with 9-month d7SSA cells restored the differentiation capacity of aged LT-HSCs to that of untreated 2-month (Figures 4C and 4D). Interestingly, although we found a significant decline in their differentiation capacity with age, there was little effect of SSA on lymphoid differentiation of LMPPs on a per-cell basis (Figures 4E and 4F). Thus, increased lymphopoiesis seems to be predicated wholly on the intrinsic increase in HSC function. Given that *Il7ra*$^{-/-}$ mice have a selective deficiency in lymphopoiesis, we would only expect limited myeloid engraftment, and indeed that was the case when we transplanted whole bone marrow (WBM) (Figures S3A and S3B). However, interestingly, when LT-HSCs were transplanted, although there was no change in engraftment of granulocytes either as a consequence of age or SSA (Figure 4G), there was a significant decrease in monocyte/macrophage reconstitution with age, which was reversed after SSA (Figure 4H).

Early Intrinsic Functional Changes in LT-HSCs

To identify whether any functional effects could be observed in HSCs earlier than day 7, 8,000–10,000 CD34-FLT3$^-$ LT-HSCs from 9-month d2SSA mice, 9-month d7SSA mice, or their shSSA controls were co-cultured with OP9-DL1 cells for 12 days. Consistent with our in vivo data, LT-HSCs derived from 9-month SSA mice progressed more rapidly to the DN2 and DN3 stages of T cell development when compared to LT-HSCs isolated from 9-month shSSA mice (Figure 5A). To explore the intrinsic mechanistic changes to the stem cell compartment after SSA, we performed transcriptome analysis on LT-HSCs from 9-month shSSA and 9-month SSA mice, 2 days after surgery. 251 genes were significantly altered ($p < 0.05$; >1.5-fold change), 55 upregulated and 196 downregulated (Figure 5B). Core pathway analysis revealed 24 genes upregulated and 13 downregulated in d7SSA LT-HSCs under the "Hematological System Development and Function" pathway (Table S1), indicating that even using an unbiased approach revealed hematopoietic-related gene changes. Upon further dissection, many of the 251 altered genes

in the spleen 70 days after transfer. (C) Concatenated flow cytometry profiles showing total donor reconstitution as well as donor Gr1$^+$CD11b$^+$ granulocyte, Gr1^{lo}CD11b$^+$ monocyte/macrophage, B220$^+$ B cells, and TCRβ$^+$ T cells reconstitution. (D) Absolute number of donor-derived cells in the periphery of *Il7ra*$^{-/-}$ recipients.

(E and F) 2,000 LMPPs from untreated CD45.1$^+$ 2-month; CD45.1$^+$ 9-month d7shSSA); or CD45.1$^+$ 9-month d7SSA were transferred into unablated 2-month *Il7ra*$^{-/-}$ recipients (n = 6 recipient/donor groups) and donor-derived hematopoiesis measured in the spleen 70 days after transfer. (E) Concatenated flow cytometry profiles showing total donor reconstitution as well as donor B220$^+$ B cells, and TCRβ$^+$ T cells reconstitution. (F) Absolute number of donor-derived cells in the periphery of *Il7ra*$^{-/-}$ recipients.

(G) Concatenated flow cytometry plots displaying donor reconstitution and absolute numbers of donor Gr1$^+$CD11b$^+$ granulocytes.

(H) Concatenated flow cytometry plots displaying donor reconstitution and absolute numbers of donor Gr1^{lo}CD11b$^+$ monocyte/macrophages.

Results are expressed as mean ± SEM. *$p < 0.05$, **$p < 0.01$, ***$p < 0.001$. See also Figure S3.

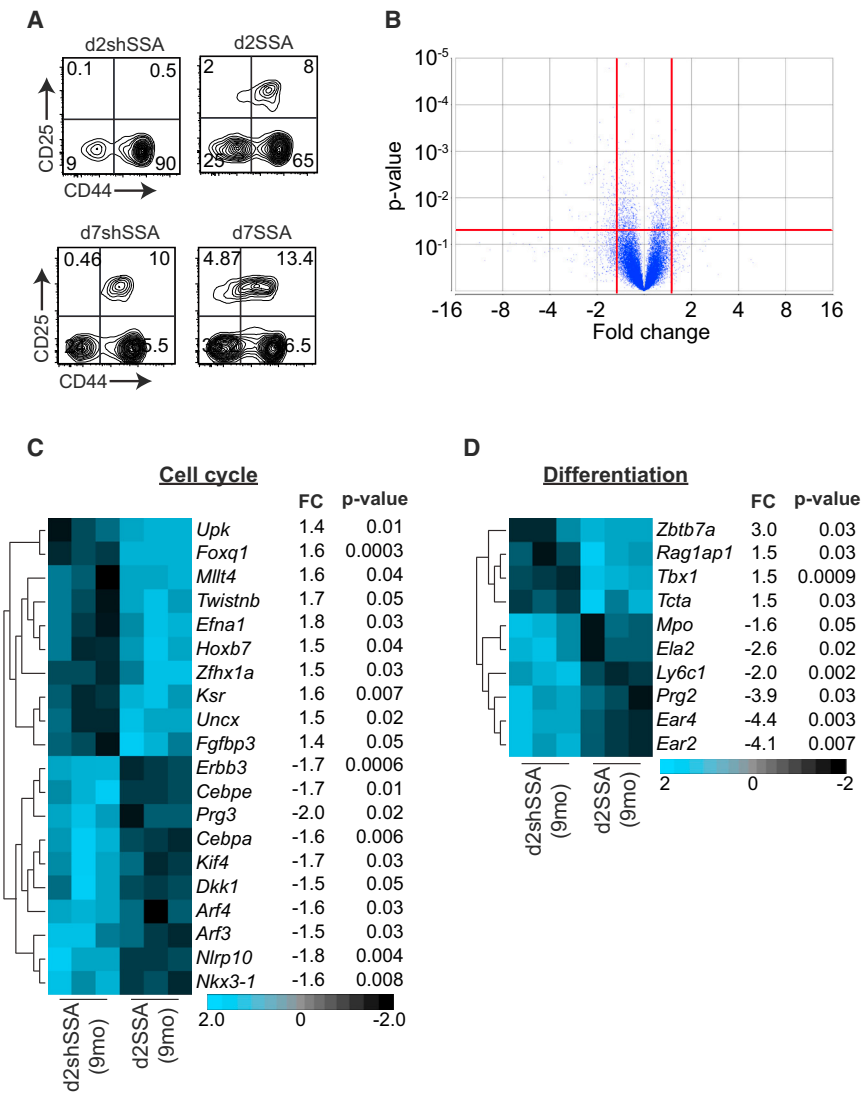

Figure 5. Intrinsic Molecular Changes within HSCs after SSA

(A) 10,000 LT-HSCs from 9-month shSSA or 9-month SSA mice 2 or 7 days after surgery were plated onto OP9-DL1 cells and T cell differentiation assessed at day 12. Concatenated FACS plots gated on $CD4^{-}CD8^{-}CD3^{-}$. (B–D) LT-HSCs from 9-month d2shSSA or 9-month d2SSA mice were FACS purified, and transcriptome analysis was performed (n = 3 biological replicates, where each replicate included cells pooled from 10–20 animals). (B) Volcano plot outlining gene expression between 9-month d2shSSA and 9-month d2SSA LT-HSCs. 251 genes were significantly altered ($p < 0.05$; >1.5-fold change), 55 upregulated and 196 downregulated. (C and D) Significant changes between 9-month d2shSSA and 9-month d2SSA LT-HSCs in genes involved with cell-cycle regulation (C) or differentiation (D).

could be broadly grouped into those that impacted on cell cycle and cell differentiation (Figures 5C and 5D), including downregulation of cell-cycle inhibitors such as ARF proteins *Nkx3-1*, *Dkk1*, and *Cebpa* and pro-apoptotic factors including *Cebpe*, *Prg3*, and *Nlrp10*. There was also an upregulation of genes promoting proliferation such as *Foxq1*, *Hoxb7*, *Zfhx1a*, and *Fgfbp3*. Consistent with the marked shift in lineage differentiation potential of HSCs with age, previous studies have found considerable gene usage skewing in HSCs from old mice away from lymphoid-associated and toward myeloid-associated genes (Rossi et al., 2005). We found that as early as day 2 after SSA, there was a significant decrease in genes associated with myeloid differentiation (*Prg2*, *Ela2*, *Mpo*, and *Ear-2, -4*) as well as upregulation of genes previously associated with lymphopoiesis (*Zbtb7a*, *Rag1ap1*, *Tbx1*, and *Tcta*) (Figure 5D).

SSA Alters Intrinsic Gene Expression by Hematopoietic Niche Cells

Given the intimate relationship between HSCs and their microenvironment, we performed transcriptome analysis on non-hematopoietic cells from the sinusoidal niche of 2- and 9-month untreated mice, 9-month shSSA, and 9-month SSA mice at days 2, 4, 7, and 10 post-SSA. 160 genes were downregulated and 72 upregulated (>2-fold) between untreated 2- and 9-month mice (Figure S4A). Of the 160 downregulated genes, pattern discovery (correlation >0.7) revealed 116 that became progressively more similar after SSA to untreated 2-month mice (Figure 6A; Table S2). Genes of note following this pattern included *Spib*, which can be induced by RANKL, a factor critical for osteoblast (OBL) differentiation (de Lau et al., 2012; Wilson, 2011); *Lgr5*, which marks stem cells in the intestine, liver, and ovary (Koo and Clevers, 2014); and *Foxo1*, which

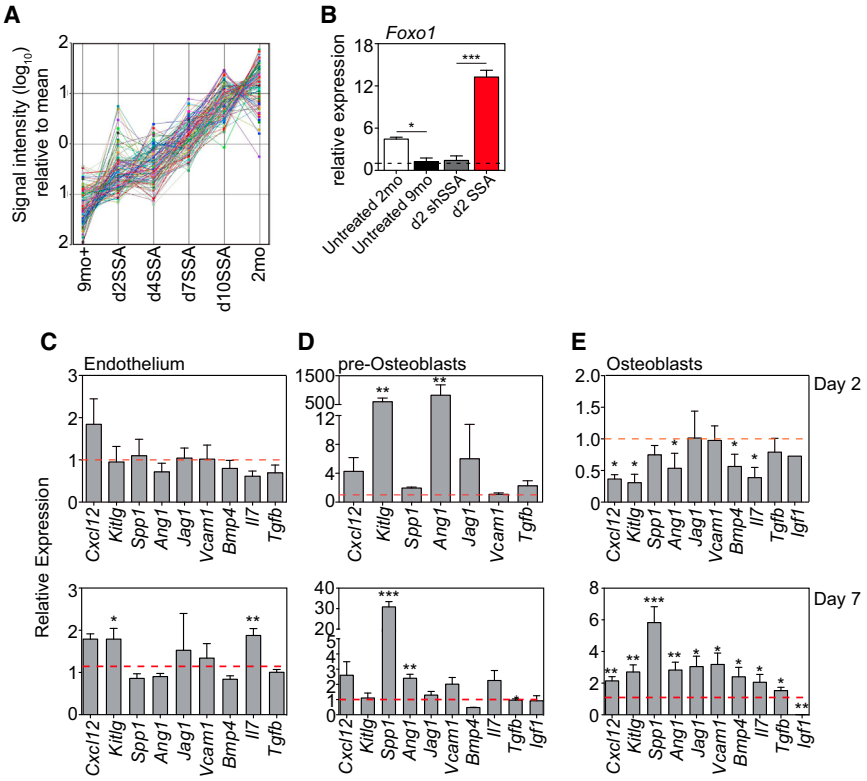

Figure 6. SSA Induces Molecular Changes to the Niche and Its Ability to Support Hematopoiesis

Transcriptome analysis was performed on purified sinusoidal CD45$^-$TER119$^-$ cells from 2- and 9-month untreated mice, 9-month shSSA control, and 9-month SSA mice at days 2, 4, 7, and 10 after surgery (n = 1, ten mice pooled/sample).

(A) Pattern discovery (correlation >0.7) identified 132 probes that demonstrated an increasing gene expression trend toward young profiles following castration of middle-aged mice.

(B) qPCR of *Foxo1* expression in pre-OBLs purified from untreated 2- or 9-month mice, and 9-month d2shSSA or 9-month d2SSA mice.

(C–E) Expression of *Cxcl12*, *Kitlg*, *Spp1*, *Ang1*, *Jag1*, *Vcam1*, *Bmp4*, *Il7*, *Tgfb*, and *Igf1* in endothelial cells (C), pre-OBLs (D), and OBLs (E) from 9-month d2SSA and 9-month d7SSA. Expression is represented as 9-month d7SSA relative to 9-month d7shSSA control mice, n = 3–11 independent experiments.

*p < 0.05, **p < 0.01, ***p < 0.001. See also Figure S4.

has been implicated in protection from age-associated pathologies in other tissues (van der Horst and Burgering, 2007). qPCR of highly purified niche subsets confirmed an increase in *Foxo1* expression by pre-OBLs as early as day 2 after SSA (Figure 6B). Gene ontology analysis of the 116-gene cluster revealed 50 Kyoto Encyclopedia of Genes and Genomes (KEGG) pathways (Figure S4B), including (1) gap junction molecules, which have been found to regulate hematopoiesis and prevent HSC senescence (Schajnovitz et al., 2011; Taniguchi Ishikawa et al., 2012), (2) cell adhesion molecule-associated pathways, which modulate the interaction of HSCs with their stromal niche (Mendelson and Frenette, 2014), and (3) the MAPK signaling pathway, which regulates the balance between HSC expansion, survival, and differentiation and has also been implicated in promoting thymopoiesis (Geest and Coffer, 2009).

To further probe the basis underlying SSA-mediated changes to HSC function, molecular changes to genes previously implicated with maintenance of hematopoietic function were examined within specific isolated niche populations. Endothelial cells (CD45$^-$TER119$^-$CD31$^+$) and pre-OBLs (CD45$^-$TER119$^-$CD31$^-$CD51$^+$) were isolated from the sinusoidal compartment after flushing bones while mature endosteal niche OBLs (CD45$^-$TER119$^-$CD31$^-$CD51$^+$) were obtained by digesting bone fragments with collagenase. Precursor status of sinusoidal-resident OBLs was confirmed by their expression of *Runx2* and their reduced expression of *Gpnb* (Osteoactivin), *Bglap* (Osteocalcin), and *Spp1* (Osteopontin), compared with endosteal OBLs (Figure S4C); consistent with data suggesting that CD51$^+$PDGFRα^+ cells in the sinusoidal niche correspond with HSC niche-forming Nestin$^+$ mesenchymal stromal cells (Pinho et al., 2013). Analysis revealed no significant changes in niche population size with age or SSA (data not shown). Although there was no notable difference in endothelial gene expression at d2SSA (9 month), there was a significant increase in the expression of *Kitlg* and *Il7* by day 7 (Figure 6C), both of which could aid in lymphoid differentiation. Within the pre-OBL population, there was a large early transient increase in *Scf* expression and *Angiopoietin-1* (*Ang-1*) at day 2, which subsided by day 7 (Figure 6D). Despite sinusoidal niche-residing pre-OBLs expressing a fraction of the *Opn* compared to endosteal OBLs on a per-cell basis (Figure S4C), 7 days following SSA sinusoidal pre-OBLs showed a 30-fold increase in Opn production compared to shSSA control mice. Within the mature endosteal OBL population, there was an initial decline in the expression of *Cxcl12*, *Scf*, *Angpt1*, *Bmp4*, and *Il7* at day 2. However, by day 7 there was a significant increase in many of these factors including *Spp1*, *Ang1*, *Cxcl12*, *Kitlg*, *Jag1*, *Vcam1*, *Bmp4*, and *Tgfb* as well as decreased *Igf1* (Figure 6E).

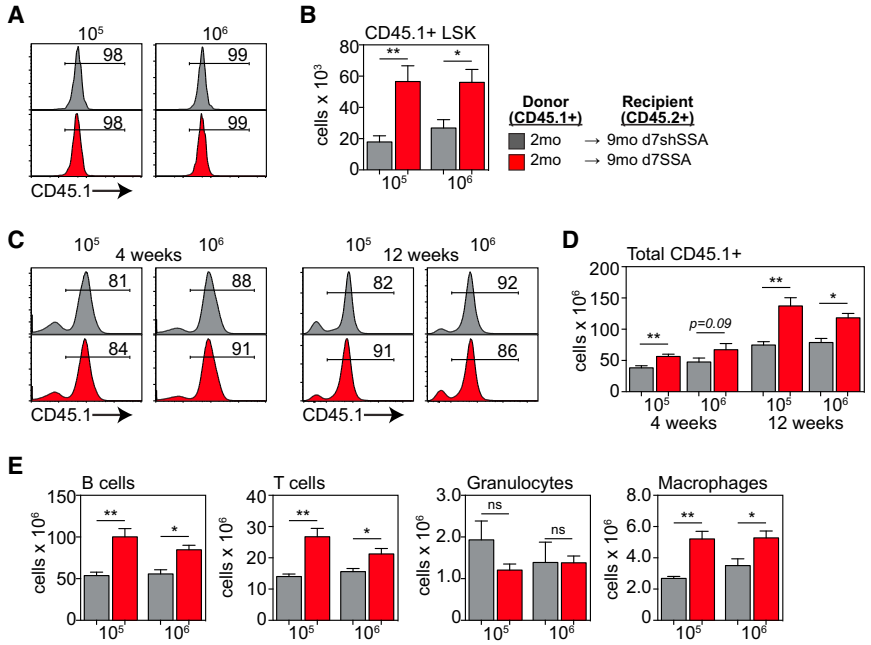

Figure 7. SSA Promotes the Ability of the Niche to Support Hematopoiesis

Lethally irradiated 9-month d7shSSA or 9-month d7SSA were reconstituted with either 5 × 10^5 or 5 × 10^6 BM cells from untreated 2-month CD45.1 donors (n = 5–6/group).

(A) Concatenated flow cytometry plots showing the proportion of donor LSK cells at 28 days after transplant.

(B) Absolute number of donor-derived LSK cells in the BM 28 days after transplant.

(C) Concatenated flow cytometry plots showing total donor reconstitution in the spleen at days 28 and 84 after transplant.

(D) Absolute number of donor-derived cells in the spleen at days 28 and 84 after transplant.

(E) Absolute number of donor-derived $Gr1^+$ $CD11b^+$ granulocyte, $Gr1^{lo}CD11b^+$ monocyte/macrophage, $B220^+$ B cells, and $TCR\beta^+$ T cells in the spleen 84 days after transplant. Results are expressed as mean ± SEM. *p < 0.05, **p < 0.01.

SSA Mediates Regeneration of the Hematopoietic Niche to Promote Lymphopoiesis

Consistent with these molecular changes in niche function, 9-month SSA-treated recipients of untreated 2-month HSCT had significantly greater engraftment of LSK cells compared with 9-month shSSA control recipients, even with ten times fewer cells transplanted (Figures 7A and 7B). This engraftment was reflected in the periphery at 4 and 12 weeks after transplant where there was an increased total number of donor cells (Figures 7C and 7D). In addition, the number of donor T cells, B cells, and macrophages was also significantly increased in recipients that had been given SSA regardless of which dose of cells they were given (Figure 7E). However, interestingly, within the granulocyte population we could detect no difference in engraftment in mice regardless of their SSA status or cell dose infused (Figure 7E). This suggests that, in addition to enhancing HSC function, SSA also enhances the function of the niche and its ability to support hematopoiesis.

DISCUSSION

One of the hallmarks of aging is reduced generation of new lymphocytes. Although there is a profound decline in the number of lymphoid progenitors with age (Min et al., 2004, 2006) that can be reversed by SSA, consistent with their sensitivity to sex steroids (Medina et al., 2001), we have demonstrated here and in previous work that the function of lymphoid progenitors does not change on a per-cell basis after SSA (Heng et al., 2005). Rather, upstream HSCs exhibit improved overall function early after the cessation of testosterone production. One hypothesis that may explain this early functional shift would be an immediate and direct intrinsic impact on stem and progenitor cells due to the removal of the negative influences of sex steroids. This was supported by the early molecular and functional changes within a highly purified population of LT-HSCs 2 days after SSA. Noteworthy among the altered genes in LT-HSCs post-SSA were downregulation of *Dkk1*, a wnt inhibitor that can be upregulated by androgens and mediate aging degeneration (Kwack et al., 2008; Seib et al., 2013); decreased *Erbb3*, elevated levels of which correlate with androgen-responsive prostate cancers (Koumakpayi et al., 2006); increased expression of *Efna1*, which has been implicated in enhanced proliferation and is downregulated upon exposure to androgens (Nantermet et al., 2004); decreased *Arf3* and *Arf4*, which have been implicated in regulating CDC42 (Erickson et al., 1996), a potential mediator of HSC aging and regeneration (Florian et al., 2012); upregulation of genes directly involved with lymphoid differentiation, such as *Zbtb7a*, *Tbx1*, and *Rag1ap1* (Gennery, 2012; Maeda et al., 2007); and downregulation of *Ear2*, which has recently been described as a negative regulator of T cell development (Ichim et al., 2014).

In our previous studies, we demonstrated that after SSA there is a significant increase in the number of all developing B and T cell subsets (Dudakov et al., 2009a, 2009b; Goldberg et al., 2010; Heng et al., 2005; Sutherland et al., 2005). However, in this study there was a clear increase in

B lymphopoiesis, while thymopoiesis was only sometimes increased. Both T and B lymphopoiesis occur in very close contact with their respective stromal microenvironments; however, T cell development is entirely dependent on these interactions, while some B lymphopoiesis can be achieved independently of the BM stromal microenvironment (Carsetti, 2000; Nagasawa, 2006; Takahama, 2006). Therefore, one hypothesis could be that altering the intrinsic function of HSCs—although enough to profoundly impact on B lymphopoiesis—is not sufficient to promote thymopoiesis, which may require additional stimulation of the stromal microenvironment. Consistent with this hypothesis, increases after SSA in T-lineage progenitors such as LMPP and CLP were not by themselves enough to promote increased thymopoiesis, without additional impact on the thymic stromal microenvironment.

In addition to intrinsic changes in HSCs, we also found a qualitative change to the BM niche, which likely contributes to the improved function of HSCs after SSA. Consistent with this, we have previously found that SSA can significantly improve hematopoietic reconstitution after HSCT (Goldberg et al., 2005, 2007, 2009), and here we could demonstrate that fewer cells were needed for effective engraftment. There is some rationale for these findings, as (1) exposure of aged satellite stem cells to a young microenvironment reverses their age-related changes (Conboy et al., 2005), and (2) subsequently several studies have reported that circulating factors in young mice can reverse age-related defects in a number of tissues including heart, brain, and skeletal muscle (Loffredo et al., 2013; Sinha et al., 2014; Villeda et al., 2014). Pattern analysis of the changed genes within the stromal microenvironment revealed a distinct shift in gene expression after SSA from a profile characteristic of an aged mouse to that of the young by d10 after SSA. Of particular interest within this group was the gene *Foxo1*, which has been described in the development and differentiation of OBLs, regulating their expression of *Runx2* and *Bglap* (Teixeira et al., 2010; Yang et al., 2011), and preventing differentiation of mesenchymal progenitor cells into fat or muscle (Nakae et al., 2003). *Foxo1* has also been implicated with protection during aging (van der Horst and Burgering, 2007), with *Foxo1*-deficient mice displaying aberrant hematopoietic phenotypes resembling those seen with age; however, it is unclear whether these are intrinsic to HSCs or mediated through the BM microenvironment (Kim et al., 2008; Tothova et al., 2007). Consistent with these changes after SSA, the androgen receptor can directly bind the *Foxo1* promoter and regulate its action, and FOXO1 can inhibit androgen receptor transcription (Liu et al., 2008; Ma et al., 2009). In addition, IGF-1, expression of which is almost completely abrogated after SSA, triggers the inactivation of FOXO1 by nuclear exclusion (Yang et al., 2011). Analysis of known hematopoietic niche interactions (Mercier et al., 2012) revealed upregulation following SSA of *Spp1*, *Ang1*, *Cxcl12*, *Kitlg* (*Scf*), *Tgfb*, *Jag1*, and *Vcam1*—many of which can be directly regulated by FOXO1 (Ferdous et al., 2011; Martinez et al., 2008; Potente et al., 2005).

Taken together, these data indicate that the widespread downstream impacts of SSA on lymphopoiesis are at least partially attributable to the considerable effects on primitive HSC function, thereby demonstrating mechanisms by which lymphopoiesis can be rejuvenated following SSA. Given that SSA can be achieved clinically, and reversibly, using currently approved agonists and antagonists of the sex steroid pathway (e.g., LHRH/GnRH), and that these improve immune function (Goldberg et al., 2009; Velardi et al., 2014), it has important implications for replenishing the diminished repertoire of lymphoid cells following damaging cytoablative treatments associated with bone marrow transplantation and cancer therapies. While the capacity for long-term BM regeneration following SSA has not yet been established, this work provides the basis for more detailed investigations into hematopoietic niche aging and SSA-induced rejuvenation, to develop more targeted strategies for HSC recovery.

EXPERIMENTAL PROCEDURES

Animals

Young (2 months) or middle-aged (9 months) male C57Bl/6 or Ly5.1 mice were obtained from the Animal Resources Centre or Monash Animal Services. *Il7ra*$^{-/-}$ mice were kindly provided by A. Strasser (Walter and Eliza Hall Institute, Melbourne). All animal experimentation was carried out at Monash University in accordance with animal experiment ethics committee guidelines. Surgical removal of the testes was performed on male mice as previously described (Heng et al., 2005). Recipient mice were lethally irradiated with 1,100-cGy total body irradiation (^{137}Cs source) as a split dose (2 × 550 cGy) separated by 3 hr and provided with antibiotics (Baytril) in water for 2 weeks after transplantation.

Cell Isolation and Analysis

Cell suspensions of the sinusoidal compartment were obtained by flushing tibias and femurs. Absolute numbers were calculated based on the total numbers of viable nucleated cells harvested from two tibias and two femurs. Osteoblasts from the endosteal niche were isolated by crushing flushed bones and digesting with 0.3% (w/v) Collagenase/Dispase (Roche) and 0.1% (w/v) DNase I (Roche) in RPMI-1640. Flow cytometric analysis and sorting was performed on FACSCalibur, FACSCanto II, FACSVantage, FACSAria, or Influx (BD Biosciences) cytometers and cell sorters. Gates were typically set using appropriate isotype controls.

Microarray and qPCR Analysis

Microarrays and bioinformatics were performed at the Australian Genome Research Facility (AGRF) using Partek v.6.5. Pathway.

Analysis on LT-HSCs was conducted using Ingenuity Pathway Analysis (IPA) software. qPCR was performed using Platinum SYBR Green Supermix-UDG (Invitrogen) on a Corbett Rotor-Gene 3000 (Corbett Research). Relative levels of target mRNA was compared to GAPDH using the $2^{-\Delta\Delta Ct}$ method, comparing 9-month d7SSA mice to 9-month d7shSSA control mice.

Statistical Analysis

Statistical analysis was performed using nonparametric, unpaired Mann-Whitney U test. Limiting dilution CRU frequencies were calculated by L-calc software (STEMCELL Technologies), using Poisson statistics (two-tailed test). Comparative analysis of relative gene expression in SSA mice was performed using Student's t test.

ACCESSION NUMBERS

The NCBI GEO accession number for gene expression data reported in this paper is GSE64841.

SUPPLEMENTAL INFORMATION

Supplemental Information includes Supplemental Experimental Procedures, four figures, and two tables and can be found with this article online at http://dx.doi.org/10.1016/j.stemcr.2015.01.018.

AUTHOR CONTRIBUTIONS

A.P.C., R.L.B., and J.A.D. conceived the studies. A.P.C., R.L.B., J.A.D., and D.M.K. designed experiments and analyzed data, with intellectual input from G.L.G. and M.R.M.v.d.B. All experiments were performed at Monash University by D.M.K., J.A.D., and M.V.H., with assistance from M.I.J., S.M.L.K., T.U., L.S., and L.F.Y. The manuscript was written and prepared by J.A.D., D.M.K., and A.P.C. with assistance from R.L.B.

ACKNOWLEDGMENTS

We acknowledge Jade Homann, Luciana Thompson, and Jade Barbuto for surgery and animal handling; Monash and AMREP core facilities for expert cell sorting; the Australian Genome Research Facility (AGRF) for bioinformatics analyses; and Mark Malin for helpful discussions. This study was funded by grants from the Australian Stem Cell Centre and the Australian National Health and Medical Research Council. J.A.D. was supported by a CJ Martin overseas biomedical training fellowship from the Australian National Health and Medical Research Council; a Scholar Award from the American Society of Hematology; and a K99/R00 Pathway to Independence Award from the NIH (K99-CA176376).

Received: August 31, 2014
Revised: January 24, 2015
Accepted: January 26, 2015
Published: February 26, 2015

REFERENCES

Carsetti, R. (2000). The development of B cells in the bone marrow is controlled by the balance between cell-autonomous mechanisms and signals from the microenvironment. J. Exp. Med. *191*, 5–8.

Chinn, I.K., Blackburn, C.C., Manley, N.R., and Sempowski, G.D. (2012). Changes in primary lymphoid organs with aging. Semin. Immunol. *24*, 309–320.

Conboy, I.M., Conboy, M.J., Wagers, A.J., Girma, E.R., Weissman, I.L., and Rando, T.A. (2005). Rejuvenation of aged progenitor cells by exposure to a young systemic environment. Nature *433*, 760–764.

de Lau, W., Kujala, P., Schneeberger, K., Middendorp, S., Li, V.S., Barker, N., Martens, A., Hofhuis, F., DeKoter, R.P., Peters, P.J., et al. (2012). Peyer's patch M cells derived from Lgr5(+) stem cells require SpiB and are induced by RankL in cultured "miniguts". Mol. Cell. Biol. *32*, 3639–3647.

Dorshkind, K., Montecino-Rodriguez, E., and Signer, R.A.J. (2009). The ageing immune system: is it ever too old to become young again? Nat. Rev. Immunol. *9*, 57–62.

Dudakov, J.A., Goldberg, G.L., Reiseger, J.J., Chidgey, A.P., and Boyd, R.L. (2009a). Withdrawal of sex steroids reverses age- and chemotherapy-related defects in bone marrow lymphopoiesis. J. Immunol. *182*, 6247–6260.

Dudakov, J.A., Goldberg, G.L., Reiseger, J.J., Vlahos, K., Chidgey, A.P., and Boyd, R.L. (2009b). Sex steroid ablation enhances hematopoietic recovery following cytotoxic antineoplastic therapy in aged mice. J. Immunol. *183*, 7084–7094.

Dykstra, B., Olthof, S., Schreuder, J., Ritsema, M., and de Haan, G. (2011). Clonal analysis reveals multiple functional defects of aged murine hematopoietic stem cells. J. Exp. Med. *208*, 2691–2703.

Erickson, J.W., Zhang, Cj., Kahn, R.A., Evans, T., and Cerione, R.A. (1996). Mammalian Cdc42 is a brefeldin A-sensitive component of the Golgi apparatus. J. Biol. Chem. *271*, 26850–26854.

Ferdous, A., Morris, J., Abedin, M.J., Collins, S., Richardson, J.A., and Hill, J.A. (2011). Forkhead factor FoxO1 is essential for placental morphogenesis in the developing embryo. Proc. Natl. Acad. Sci. USA *108*, 16307–16312.

Florian, M.C., Dörr, K., Niebel, A., Daria, D., Schrezenmeier, H., Rojewski, M., Filippi, M.-D., Hasenberg, A., Gunzer, M., Scharffetter-Kochanek, K., et al. (2012). Cdc42 activity regulates hematopoietic stem cell aging and rejuvenation. Cell Stem Cell *10*, 520–530.

Geest, C.R., and Coffer, P.J. (2009). MAPK signaling pathways in the regulation of hematopoiesis. J. Leukoc. Biol. *86*, 237–250.

Geiger, H., de Haan, G., and Florian, M.C. (2013). The ageing haematopoietic stem cell compartment. Nat. Rev. Immunol. *13*, 376–389.

Gennery, A.R. (2012). Immunological aspects of 22q11.2 deletion syndrome. Cell. Mol. Life Sci. *69*, 17–27.

Goldberg, G.L., Sutherland, J.S., Hammet, M.V., Milton, M.K., Heng, T.S., Chidgey, A.P., and Boyd, R.L. (2005). Sex steroid ablation enhances lymphoid recovery following autologous hematopoietic stem cell transplantation. Transplantation *80*, 1604–1613.

Goldberg, G.L., Alpdogan, O., Muriglan, S.J., Hammett, M.V., Milton, M.K., Eng, J.M., Hubbard, V.M., Kochman, A., Willis, L.M., Greenberg, A.S., et al. (2007). Enhanced immune reconstitution by sex steroid ablation following allogeneic hemopoietic stem cell transplantation. J. Immunol. *178*, 7473–7484.

Goldberg, G.L., King, C.G., Nejat, R.A., Suh, D.Y., Smith, O.M., Bretz, J.C., Samstein, R.M., Dudakov, J.A., Chidgey, A.P., Chen-Kiang, S., et al. (2009). Luteinizing hormone-releasing hormone enhances T cell recovery following allogeneic bone marrow transplantation. J. Immunol. *182*, 5846–5854.

Goldberg, G.L., Dudakov, J.A., Reiseger, J.J., Seach, N., Ueno, T., Vlahos, K., Hammett, M.V., Young, L.F., Heng, T.S.P., Boyd, R.L., and Chidgey, A.P. (2010). Sex steroid ablation enhances immune reconstitution following cytotoxic antineoplastic therapy in young mice. J. Immunol. *184*, 6014–6024.

Gossens, K., Naus, S., Corbel, S.Y., Lin, S., Rossi, F.M.V., Kast, J., and Ziltener, H.J. (2009). Thymic progenitor homing and lymphocyte homeostasis are linked via S1P-controlled expression of thymic P-selectin/CCL25. J. Exp. Med. *206*, 761–778.

Heng, T.S., Goldberg, G.L., Gray, D.H., Sutherland, J.S., Chidgey, A.P., and Boyd, R.L. (2005). Effects of castration on thymocyte development in two different models of thymic involution. J. Immunol. *175*, 2982–2993.

Ichim, C.V., Dervović, D.D., Zúñiga-Pflücker, J.C., and Wells, R.A. (2014). The orphan nuclear receptor Ear-2 (Nr2f6) is a novel negative regulator of T cell development. Exp. Hematol. *42*, 46–58.

Kim, D.H., Kim, J.Y., Yu, B.P., and Chung, H.Y. (2008). The activation of NF-kappaB through Akt-induced FOXO1 phosphorylation during aging and its modulation by calorie restriction. Biogerontology *9*, 33–47.

Koo, B.K., and Clevers, H. (2014). Stem cells marked by the R-spondin receptor LGR5. Gastroenterology *147*, 289–302.

Koumakpayi, I.H., Diallo, J.S., Le Page, C., Lessard, L., Gleave, M., Bégin, L.R., Mes-Masson, A.M., and Saad, F. (2006). Expression and nuclear localization of ErbB3 in prostate cancer. Clin. Cancer Res. *12*, 2730–2737.

Kwack, M.H., Sung, Y.K., Chung, E.J., Im, S.U., Ahn, J.S., Kim, M.K., and Kim, J.C. (2008). Dihydrotestosterone-inducible dickkopf 1 from balding dermal papilla cells causes apoptosis in follicular keratinocytes. J. Invest. Dermatol. *128*, 262–269.

Liang, Y., Van Zant, G., and Szilvassy, S.J. (2005). Effects of aging on the homing and engraftment of murine hematopoietic stem and progenitor cells. Blood *106*, 1479–1487.

Liu, P., Li, S., Gan, L., Kao, T.P., and Huang, H. (2008). A transcription-independent function of FOXO1 in inhibition of androgen-independent activation of the androgen receptor in prostate cancer cells. Cancer Res. *68*, 10290–10299.

Loffredo, F.S., Steinhauser, M.L., Jay, S.M., Gannon, J., Pancoast, J.R., Yalamanchi, P., Sinha, M., Dall'Osso, C., Khong, D., Shadrach, J.L., et al. (2013). Growth differentiation factor 11 is a circulating factor that reverses age-related cardiac hypertrophy. Cell *153*, 828–839.

Ma, Q., Fu, W., Li, P., Nicosia, S.V., Jenster, G., Zhang, X., and Bai, W. (2009). FoxO1 mediates PTEN suppression of androgen receptor N- and C-terminal interactions and coactivator recruitment. Mol. Endocrinol. *23*, 213–225.

Maeda, T., Merghoub, T., Hobbs, R.M., Dong, L., Maeda, M., Zakrzewski, J., van den Brink, M.R.M., Zelent, A., Shigematsu, H., Akashi, K., et al. (2007). Regulation of B versus T lymphoid lineage fate decision by the proto-oncogene LRF. Science *316*, 860–866.

Martinez, S.C., Tanabe, K., Cras-Méneur, C., Abumrad, N.A., Bernal-Mizrachi, E., and Permutt, M.A. (2008). Inhibition of Foxo1 protects pancreatic islet beta-cells against fatty acid and endoplasmic reticulum stress-induced apoptosis. Diabetes *57*, 846–859.

Medina, K.L., Garrett, K.P., Thompson, L.F., Rossi, M.I., Payne, K.J., and Kincade, P.W. (2001). Identification of very early lymphoid precursors in bone marrow and their regulation by estrogen. Nat. Immunol. *2*, 718–724.

Mendelson, A., and Frenette, P.S. (2014). Hematopoietic stem cell niche maintenance during homeostasis and regeneration. Nat. Med. *20*, 833–846.

Mercier, F.E., Ragu, C., and Scadden, D.T. (2012). The bone marrow at the crossroads of blood and immunity. Nat. Rev. Immunol. *12*, 49–60.

Miller, J.P., and Allman, D. (2003). The decline in B lymphopoiesis in aged mice reflects loss of very early B-lineage precursors. J. Immunol. *171*, 2326–2330.

Min, H., Montecino-Rodriguez, E., and Dorshkind, K. (2004). Reduction in the developmental potential of intrathymic T cell progenitors with age. J. Immunol. *173*, 245–250.

Min, H., Montecino-Rodriguez, E., and Dorshkind, K. (2006). Effects of aging on the common lymphoid progenitor to pro-B cell transition. J. Immunol. *176*, 1007–1012.

Morrison, S.J., Wandycz, A.M., Akashi, K., Globerson, A., and Weissman, I.L. (1996). The aging of hematopoietic stem cells. Nat. Med. *2*, 1011–1016.

Nagasawa, T. (2006). Microenvironmental niches in the bone marrow required for B-cell development. Nat. Rev. Immunol. *6*, 107–116.

Nakada, D., Oguro, H., Levi, B.P., Ryan, N., Kitano, A., Saitoh, Y., Takeichi, M., Wendt, G.R., and Morrison, S.J. (2014). Oestrogen increases haematopoietic stem-cell self-renewal in females and during pregnancy. Nature *505*, 555–558.

Nakae, J., Kitamura, T., Kitamura, Y., Biggs, W.H., 3rd, Arden, K.C., and Accili, D. (2003). The forkhead transcription factor Foxo1 regulates adipocyte differentiation. Dev. Cell *4*, 119–129.

Nantermet, P.V., Xu, J., Yu, Y., Hodor, P., Holder, D., Adamski, S., Gentile, M.A., Kimmel, D.B., Harada, S., Gerhold, D., et al. (2004). Identification of genetic pathways activated by the androgen receptor during the induction of proliferation in the ventral prostate gland. J. Biol. Chem. *279*, 1310–1322.

Pinho, S., Lacombe, J., Hanoun, M., Mizoguchi, T., Bruns, I., Kunisaki, Y., and Frenette, P.S. (2013). PDGFRα and CD51 mark human nestin+ sphere-forming mesenchymal stem cells capable of hematopoietic progenitor cell expansion. J. Exp. Med. *210*, 1351–1367.

Potente, M., Urbich, C., Sasaki, K., Hofmann, W.K., Heeschen, C., Aicher, A., Kollipara, R., DePinho, R.A., Zeiher, A.M., and Dimmeler, S. (2005). Involvement of Foxo transcription factors in angiogenesis and postnatal neovascularization. J. Clin. Invest. *115*, 2382–2392.

Rodewald, H.R. (1998). The thymus in the age of retirement. Nature *396*, 630–631.

Rossi, D.J., Bryder, D., Zahn, J.M., Ahlenius, H., Sonu, R., Wagers, A.J., and Weissman, I.L. (2005). Cell intrinsic alterations underlie

hematopoietic stem cell aging. Proc. Natl. Acad. Sci. USA *102*, 9194–9199.

Schajnovitz, A., Itkin, T., D'Uva, G., Kalinkovich, A., Golan, K., Ludin, A., Cohen, D., Shulman, Z., Avigdor, A., Nagler, A., et al. (2011). CXCL12 secretion by bone marrow stromal cells is dependent on cell contact and mediated by connexin-43 and connexin-45 gap junctions. Nat. Immunol. *12*, 391–398.

Seib, D.R., Corsini, N.S., Ellwanger, K., Plaas, C., Mateos, A., Pitzer, C., Niehrs, C., Celikel, T., and Martin-Villalba, A. (2013). Loss of Dickkopf-1 restores neurogenesis in old age and counteracts cognitive decline. Cell Stem Cell *12*, 204–214.

Sinha, M., Jang, Y.C., Oh, J., Khong, D., Wu, E.Y., Manohar, R., Miller, C., Regalado, S.G., Loffredo, F.S., Pancoast, J.R., et al. (2014). Restoring systemic GDF11 levels reverses age-related dysfunction in mouse skeletal muscle. Science *344*, 649–652.

Sutherland, J.S., Goldberg, G.L., Hammett, M.V., Uldrich, A.P., Berzins, S.P., Heng, T.S., Blazar, B.R., Millar, J.L., Malin, M.A., Chidgey, A.P., and Boyd, R.L. (2005). Activation of thymic regeneration in mice and humans following androgen blockade. J. Immunol. *175*, 2741–2753.

Takahama, Y. (2006). Journey through the thymus: stromal guides for T-cell development and selection. Nat. Rev. Immunol. *6*, 127–135.

Taniguchi Ishikawa, E., Gonzalez-Nieto, D., Ghiaur, G., Dunn, S.K., Ficker, A.M., Murali, B., Madhu, M., Gutstein, D.E., Fishman, G.I., Barrio, L.C., and Cancelas, J.A. (2012). Connexin-43 prevents hematopoietic stem cell senescence through transfer of reactive oxygen species to bone marrow stromal cells. Proc. Natl. Acad. Sci. USA *109*, 9071–9076.

Teixeira, C.C., Liu, Y., Thant, L.M., Pang, J., Palmer, G., and Alikhani, M. (2010). Foxo1, a novel regulator of osteoblast differentiation and skeletogenesis. J. Biol. Chem. *285*, 31055–31065.

Thurmond, T.S., Murante, F.G., Staples, J.E., Silverstone, A.E., Korach, K.S., and Gasiewicz, T.A. (2000). Role of estrogen receptor alpha in hematopoietic stem cell development and B lymphocyte maturation in the male mouse. Endocrinology *141*, 2309–2318.

Tothova, Z., Kollipara, R., Huntly, B.J., Lee, B.H., Castrillon, D.H., Cullen, D.E., McDowell, E.P., Lazo-Kallanian, S., Williams, I.R., Sears, C., et al. (2007). FoxOs are critical mediators of hematopoietic stem cell resistance to physiologic oxidative stress. Cell *128*, 325–339.

van der Horst, A., and Burgering, B.M. (2007). Stressing the role of FoxO proteins in lifespan and disease. Nat. Rev. Mol. Cell Biol. *8*, 440–450.

Velardi, E., Tsai, J.J., Holland, A.M., Wertheimer, T., Yu, V.W.C., Zakrzewski, J.L., Tuckett, A.Z., Singer, N.V., West, M.L., Smith, O.M., et al. (2014). Sex steroid blockade enhances thymopoiesis by modulating Notch signaling. J. Exp. Med. *211*, 2341–2349.

Villeda, S.A., Plambeck, K.E., Middeldorp, J., Castellano, J.M., Mosher, K.I., Luo, J., Smith, L.K., Bieri, G., Lin, K., Berdnik, D., et al. (2014). Young blood reverses age-related impairments in cognitive function and synaptic plasticity in mice. Nat. Med. *20*, 659–663.

Wilson, C. (2011). Osteocytes, RANKL and bone loss. Nat. Rev. Endocrinol. *7*, 693.

Woolthuis, C.M., de Haan, G., and Huls, G. (2011). Aging of hematopoietic stem cells: Intrinsic changes or micro-environmental effects? Curr. Opin. Immunol. *23*, 512–517.

Yang, S., Xu, H., Yu, S., Cao, H., Fan, J., Ge, C., Fransceschi, R.T., Dong, H.H., and Xiao, G. (2011). Foxo1 mediates insulin-like growth factor 1 (IGF1)/insulin regulation of osteocalcin expression by antagonizing Runx2 in osteoblasts. J. Biol. Chem. *286*, 19149–19158.

Stem Cell Reports

Supplemental Information

Enhanced Hematopoietic Stem Cell Function Mediates Immune Regeneration following Sex Steroid Blockade

Danika M. Khong, Jarrod A. Dudakov, Maree V. Hammett, Marc I. Jurblum, Sacha M.L. Khong, Gabrielle L. Goldberg, Tomoo Ueno, Lisa Spyroglou, Lauren F. Young, Marcel R.M. van den Brink, Richard L. Boyd, and Ann P. Chidgey

Supplemental Experimental Procedures

Flow Cytometry

The following antibodies and clones for flow cytometry were purchased from eBiosciences or BD Biosciences: CD3 (145-2C11), CD4 (GK1.5), CD8α (53-6.7), CD11b (M1/70), CD11c (HL3), CD19 (1D3), CD27 (LG.3A10), CD31 (MEC 13.3), CD34 (RAM34), CD44 (IM7), CD45 (30-F11), CD45.1 (A20), CD45.2 (104), CD45R/B220 (RA3-6B2), CD49d (9C10), CD49e (5H10-27), CD51 (RMU-7), CD61 (2C9.G2), CD62L (MEL-14), CD117 (2B8), CD135 (A2F10.1), CD184 (2B11/CXCR4), SCA1 (D7), Gr-1 (RB6-8C5) and TER119. Streptavidin-Pacific Orange was purchased from Molecular Probes. Lineage-Sca1+cKit+ (LSK) cells were divided into Long term HSC (LT-HSC; CD34-Flt3-); Short term HSC (ST-HSC; CD34+Flt3-); Multipotent Progenitors (MPP; CD34+Flt3+) cells with Lymphoid biased MPP (LMPP) being Flt3hiCD62L+. Osteoblasts were defined as CD45-TER119-CD31-CD51+ and endothelial cells as CD45-TER119-CD31+CD51-.

Transplantation Assays

Male (2mo or 9mo) mice were used for all transplant experiments. For competitive repopulation assays, donor and competitor BM or LSK were pooled and transplanted into recipients. For serial transplantation assays, donor mice were sacrificed and their BM individually suspended and transferred so that there were two primary recipients per individual donor. Primary recipients were sacrificed at 12 weeks after transplant and their BM individually suspended and

transferred so that there was one recipient per individual donor. Transplants assessing *in vivo* differentiation to *Il7ra*$^{-/-}$ recipients used whole BM or sorted LT-HSCs or LMPPs from individual donors and transplanted them into recipients such that each recipient received cells from 1 individual donor.

Microarray and qPCR analysis

Isolated RNA was amplified from purified cell populations (>99%) using the Ambion Total Prep Amplification kit and hybridized to Illumina Mouse WG-6_V2 (LT-HSCs) arrays or Affymetrix arrays (non-hematopoietic niche cells). Pre-validated primers for *Foxo1* (QT00116186); *Cxcl12* (QT00161112); *Kitlg* (QT00416353); *Spp1* (QT00157724); *Angpt1* (QT00166859); *Jag1* (QT00115703); *Vcam1* (QT00128793); *Bmp4* (QT00111174); *Il7* (QT00101318); *Tgfb1* (QT00145250); and *Igf1* (QT00154469) were purchased from Qiagen.

Figure S1

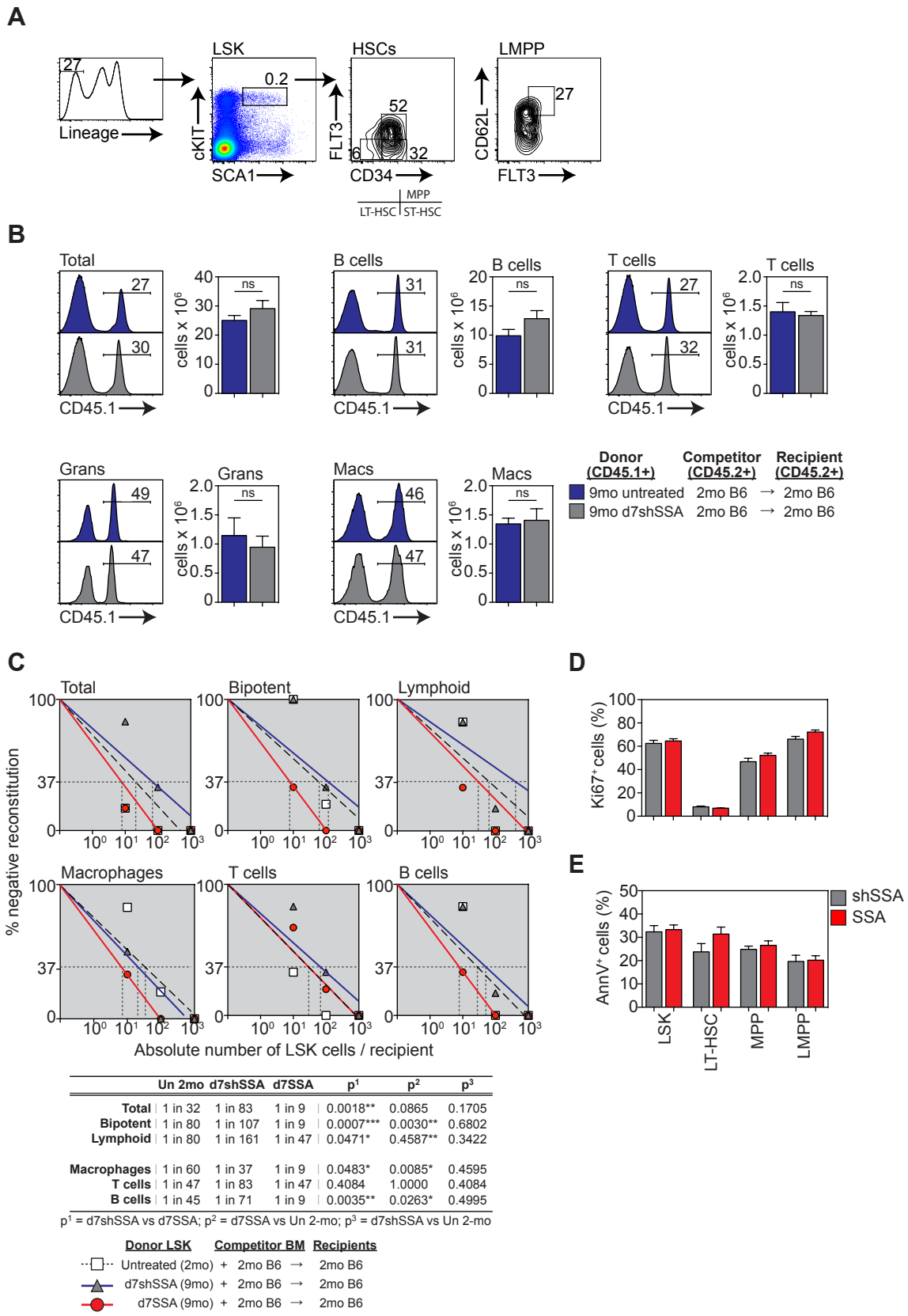

	Un 2mo	d7shSSA	d7SSA	p¹	p²	p³
Total	1 in 32	1 in 83	1 in 9	0.0018**	0.0865	0.1705
Bipotent	1 in 80	1 in 107	1 in 9	0.0007***	0.0030**	0.6802
Lymphoid	1 in 80	1 in 161	1 in 47	0.0471*	0.4587**	0.3422
Macrophages	1 in 60	1 in 37	1 in 9	0.0483*	0.0085*	0.4595
T cells	1 in 47	1 in 83	1 in 47	0.4084	1.0000	0.4084
B cells	1 in 45	1 in 71	1 in 9	0.0035**	0.0263*	0.4995

p¹ = d7shSSA vs d7SSA; p² = d7SSA vs Un 2-mo; p³ = d7shSSA vs Un 2-mo

Donor LSK	Competitor BM	Recipients
Untreated (2mo)	+ 2mo B6 →	2mo B6
d7shSSA (9mo)	+ 2mo B6 →	2mo B6
d7SSA (9mo)	+ 2mo B6 →	2mo B6

Figure S1. Gating strategies, transplantation controls and individual lineage analysis for limiting-dilution competitive repopulation assays, related to Figure 1.

(**A**). Gating strategy to identify hematopoietic stem and progenitor cells in the bone marrow. All cells expressing lineage-associated markers (CD3, CD4, CD8, B220, Gr1, CD11b, CD11c, NK1.1) were gated out and expression of ckit and Sca1 was analysed. Cells that were Lin-Sca1+ckit+ are termed LSK cells and encompass all hematopoietic stem cells as well as some of their downstream progenitors. Looking at expression of CD34 and Flt3 (CD135) on LSK cells allows the distinction between LT-HSCs, ST-HSCs and MPPs. Within the Flt3+CD34+ MPP population, cells that are skewed toward the lymphoid lineage and have considerable T cell potential, defined as LMPPs, can be identified based on expression of CD62L and high levels of Flt3 (Adolfsson et al., 2001; Adolfsson et al., 2005; Bhandoola and Sambandam, 2006; Perry et al., 2004). (**B**). 5 x 10^6 BM cells from untreated 9mo mice or 9mo mice that had undergone shSSA 7 days earlier were transplanted along with 5 x 10^6 BM cells from untreated 2mo mice into lethally irradiated (2 x 550cGy) congenic recipients. Concatenated flow cytometry plots and absolute number of total donor cells, as well as donor B220+ B cells, TCRβ+ T cells, Gr1+CD11b+ granulocytes, and Gr1^{lo}CD11b+ monocyte/macrophages was assessed 12 weeks after transplant (n=10/group). **(C)** LSK cells from untreated CD45.2$^+$ 2mo; CD45.2$^+$ 9mo animals 7 days following surgical shSSA (d7shSSA); or CD45.2$^+$ 9mo animals 7 days following surgical SSA (d7SSA) (n=6 recipients/group/dose) were FACS purified

and 10, 100 or 1000 cells were transferred into lethally irradiated congenic CD45.1 recipients along with 5 x 10^5 $CD45.1^+$ supporting BM cells. Reconstitution (>1%) was analysed 12 weeks after transplant and the frequency of repopulating cells was calculated by Poisson statistics. Parameters measured included assessing cells that gave rise to >1% total CD45.1+ cells (Total); >1% CD45.1+ B or T cells, and >1% CD45.1+ granulocytes or monocytes/macrophages (Bipotent); >1% CD45.1+ B and T cells (Lymphoid). (**D**) Proportion of $Ki67^+$ LSK cells 4, 7 and 14 days after surgical SSA in 9mo shSSA or SSA mice (n=10/treatment/timepoint). **(E)** Proportion of $Ki67^+$ cells 7 days after SSA in $CD34^-$ HSCs, $CD34^+CD62L^-$ MPPs and $CD34^+CD62L^+$ LMPPs (n=10/treatment). (**C**) Proportion of $AnnV^+$ cells 7 days after SSA in $CD34^-$ HSCs, $CD34^+CD62L^-$ MPPs and $CD34^+CD62L^+$ LMPPs (n=10/treatment). Results are expressed as mean ± SEM. *$p < 0.05$, **$p < 0.01$. * compared with 9mo shSSA mice.

Figure S2

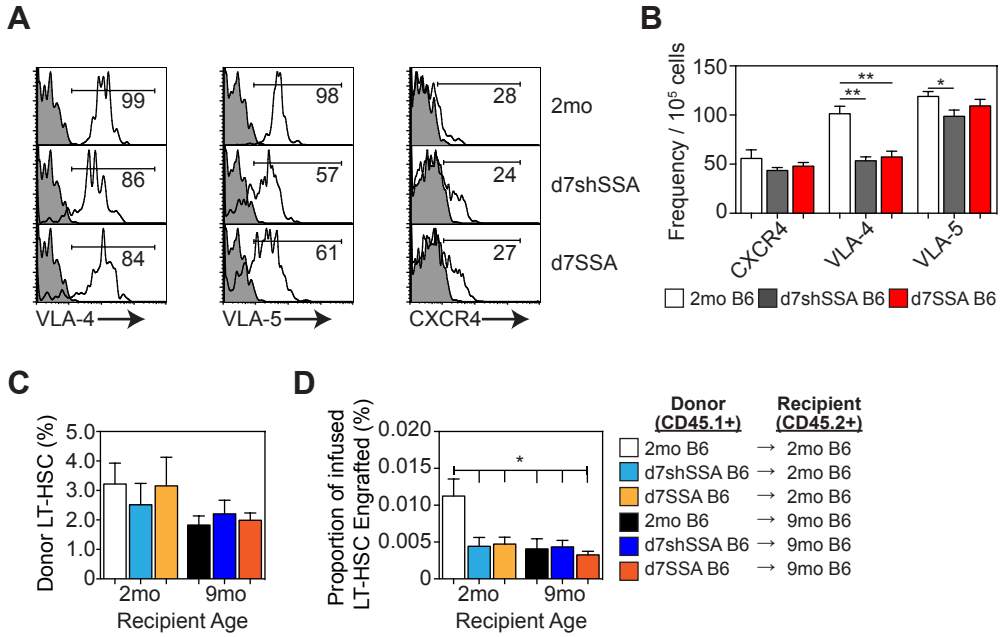
A
99
86
84
98
57
61
28
24
27
2mo
d7shSSA
d7SSA
VLA-4
VLA-5
CXCR4
B
Frequency / 10^5 cells
150
100
50
0
**
**
*
CXCR4
VLA-4
VLA-5
2mo B6
d7shSSA B6
d7SSA B6
C
Donor LT-HSC (%)
5.0
4.0
3.0
2.0
1.0
0
2mo
9mo
Recipient Age
D
Proportion of infused LT-HSC Engrafted (%)
0.020
0.015
0.010
0.005
0
*
2mo
9mo
Recipient Age
Donor (CD45.1+)
Recipient (CD45.2+)
2mo B6 → 2mo B6
d7shSSA B6 → 2mo B6
d7SSA B6 → 2mo B6
2mo B6 → 9mo B6
d7shSSA B6 → 9mo B6
d7SSA B6 → 9mo B6

Figure S2. Assessment of homing capacity of HSCs with age and after SSA, related to Figures 1 & 2.

(A) Representative FACS plots showing expression of VLA-4, VLA-5 and CXCR-4 on LSK cells from untreated 2mo; 9mo-d7shSSA; or 9mo-d7SSA. Shaded plots represent isotype controls. **(B)** Frequency of LSK cells expressing CXCR4 (n=10/treatment), VLA-4 (n=5/treatment) or VLA-5 (n=5/treatment) in vascular BM. **(C-D)** 20 x 10^6 BM cells from individual untreated CD45.1+ 2mo; $CD45.1^+$ 9mo-d7shSSA; or $CD45.1^+$ 9mo-d7SSA were transferred into unablated 2mo (n=10/donor group, one donor/recipient) or 9mo (n=10/donor group, one donor/recipient) C57Bl/6 mice. (**C**) Proportion of $CD45.1^+$ $CD34^-Flt3^-$ LT-HSCs in vascular BM 40 hours after transplant. (**D**) Engraftment was calculated relative to the number of $CD34^-Flt3^-$ LT-HSCs transferred. Results are expressed as mean ± SEM.

Figure S3

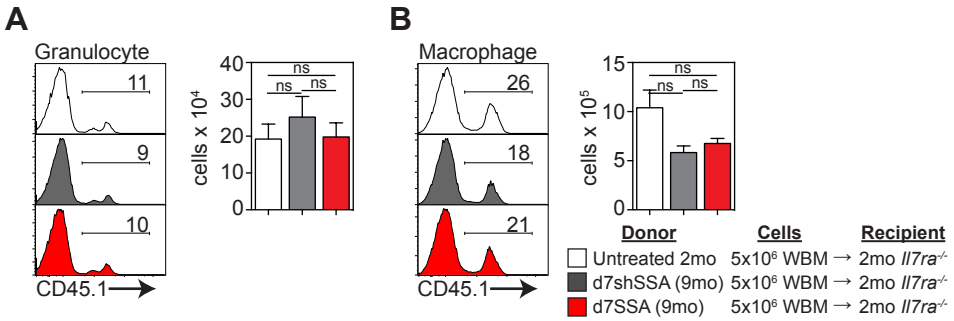
A
Granulocyte
11
9
10
CD45.1
cells x 10⁴
40
30
20
10
0
ns
ns
ns
B
Macrophage
26
18
21
CD45.1
cells x 10⁵
15
10
5
0
ns
ns
ns
Donor
Cells
Recipient
Untreated 2mo
5x10⁶ WBM → 2mo Il7ra-/-
d7shSSA (9mo)
5x10⁶ WBM → 2mo Il7ra-/-
d7SSA (9mo)
5x10⁶ WBM → 2mo Il7ra-/-

Figure S3. Myeloid reconstitution of *Il7ra*$^{-/-}$ mice, related to Figure 4.

(**A-B**) 5 x 10^6 BM cells from untreated CD45.1$^+$ 2mo; CD45.1$^+$ 9mo-d7shSSA); or CD45.1$^+$ 9mo-d7SSA were transferred into unablated 2mo *Il7ra*$^{-/-}$ recipients (n=6 recipient/donor groups, one recipient per donor). (A) Concatenated flow cytometry plots displaying donor reconstitution and absolute numbers of donor Gr1+CD11b+ granulocytes. (B) Concatenated flow cytometry plots displaying donor reconstitution and absolute numbers of donor Gr1^{lo}CD11b+ monocyte/macrophages. Results are expressed as mean ± SEM. * $p < 0.05$, ** $p < 0.01$, *** $p < 0.001$.

Figure S4

A

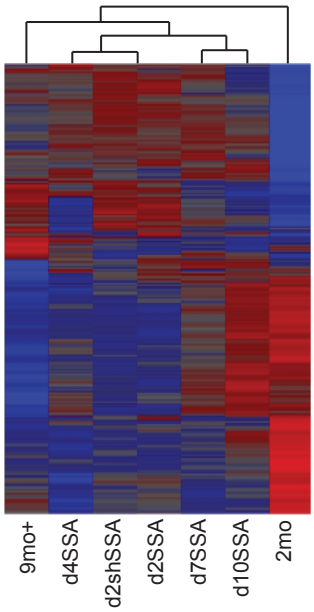

B

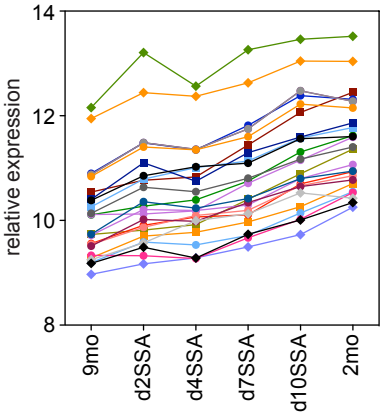

Pathway	p-value	Fold-change
Glycosaminoglycan biosynthesis	1.08E-05	-3.7424
Primary Immunodeficiency	1.09E-11	-3.0933
Hematopoietic cell lineage	3.26E-08	-2.8581
Gap Junction	0.00128	-2.8555
B cell receptor signaling pathway	2.88E-11	-2.7783
Cytokine-receptor interactions	2.19E-07	-2.7543
Phagosome	2.86E-05	-2.6765
Protein digestion and absorption	0.00312	-2.6694
Carbohydrate digestion	0.00147	-2.6366
Calcium reabsorption	0.00147	-2.6366
MAPK signaling pathway	3.69E-18	-2.5927
Chemokine signaling pathway	2.03E-05	-2.5688
Pathways in cancer	8.41E-08	-2.5575
Jak-STAT signaling pathway	0.00035	-2.5483
Spliceosome	0.00025	-2.4826
Sodium reabsorption	2.50E-05	-2.4738
Regulation of actin	0.00017	-2.4374
FcγR-mediated phagocytosis	5.03E-06	-2.4083
Metabolic pathways	1.07E-11	-2.4020
Protein processing in ER	6.04E-06	-2.3263
p53 signaling pathway	0.00124	-2.3055
T cell receptor signaling	0.00082	-2.3024
Purine metabolism	0.02712	-2.2593
Cell adhesion molecules	7.16E-06	-2.239
Glutamatergic synapse	8.43E-05	-2.1321

C

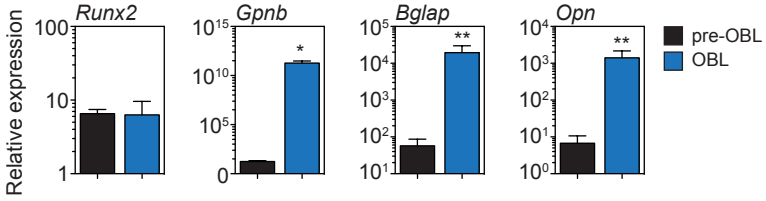

Figure S4. Cluster and pathway analysis of changed genes in, and validation of, hematopoietic niche cells, related to Figure 6.

(A) Unbiased hierarchical cluster analysis of microarray data across young, aged and early time-points (days 2-10) following shSSA or SSA. (**B**) Gene Ontology analysis of the gene cluster of 116 genes that reversed the pattern of expression between 2mo and 9mo mice after SSA. 50 KEGG pathways were revealed with 25 out of 50 KEGG pathways represented. (**C**) CD45-CD31-CD51+ osteoblastic lineage cells were FACS purified from sinusoidal (pre-OBL) or endosteal (OBL) niches. Expression of the osteoblast-related genes *Runx2*, *Gpnb* (osteoactivin), *Bglap* (osteocalcin) and *Opn* (osteopontin) were examined by qPCR. Bar graphs represent mean ± SEM of 4-6 biological replicates (where each replicate included cells pooled from 5-10 animals). Expression was measured relative to CD31+ endothelial cells isolated from the sinusoidal niche.

	Category	p-value	Genes
Upregulated	Nervous system development and function	2.0×10^{-5} – 4.99×10^{-2}	*Hexb, Cyp7b1, Pitx2, Upp1, Disp1, Palld, Rhbdf1, Csrp2, Bmp4, Efna1, Tcf7l2, Apbb1, Tardbp, Hoxb2, Clcn3, E2f5, Dst, Socs2, Cited2, Nhlrc1, Kif1b, Selp, Gpr171, Tgif1, Bbs2, Mmp24*
	Hematological System Development and Function	1.04×10^{-4} – 4.86×10^{-2}	*Clcn3, Birc2, Anxa7, Hexb, Cyp7b1, Hps6, Hivep3, Rap1gap ,Cish, Trpc6, F2rl3, Gsta4, Mfap2, Lcp2, Bst2, Selp, Serpina3g, Cd84, Arhgef1, Tnfrsf13c, Fnip1, Zbtb7a, C1galt1c1, Tbxas1*
	Cardiovascular Disease	1.72×10^{-4} – 4.99×10^{-2}	*Birc2, Anxa7, Lcp2, Gna11, Pitx2, Bmp4, Tgif1, Trpc6, F2rl3, Cited2*
	Neurological Disease	1.72×10^{-4} – 4.49×10^{-2}	*Clcn3, E2f5, Anxa7, Hexb, Pitx2, Dst, Rap1gap, Upp1, Disp1, Cited2, Mfap2, Nhlrc1, Palld,Rhbdf1, Csrp2, Selp, Bmp4, Tgif1, Mmp24, Tardbp, Hoxb2*
	Ophthalmic Disease	1.72×10^{-4} – 4.99×10^{-2}	*Clcn3, Hexb, Pitx2, Bmp4, B9d1, Cited2*
Downregulated	Inflammatory Response	1.53×10^{-4} – 4.86×10^{-2}	*Prg2, Diaph1, Als2, Mpo, Anxa3, Birc5, Ctsg, Srebf2, Hp, Fcgr2b, Cpa3, Hdc, Rgs1, Ear2*
	Cancer	1.71×10^{-4} – 4.79×10^{-2}	*Rrm2, Fancd2, Hp, Tyms, Mta1, Anxa3, Mpo,Birc5, Ilf3, Kif11, Mki67*
	Organismal Injury and Abnormalities	1.71×10^{-4} – 4.79×10^{-2}	*Top2a, Diaph1, Als2, Mta1, Mpo, Anxa3, Ctsg, Kif11, Rrm2, Fancd2, Hp, Fcgr2b, Ilf3, Tfdp1*
	Reproductive System Disease	1.71×10^{-4} – 4.79×10^{-2}	*Rrm2, Hp, Fancd2, Mta1, Anxa3, Ilf3, Kif11, Tfdp1*
	Cellular Movement	5.7×10^{-4} – 3.91×10^{-2}	*Diaph1, Als2, Hp, Fcgr2b, Rgs1, Hdc, Mpo, Ear2 , Ctsg*

Table S1 – List of the top five pathways generated by Ingenuity Pathway Analysis (IPA) from genes upregulated or downregulayed in LT-HSC purified from d2SSA compared to LT-HSC purified from d2ShSSA controls (p-value $\geq$ 0.05, fold change $\geq$ +/-1.5). Microarray analysis was performed on 3 biological replicates from each group.

1	1700027N10Rik	30	D930015E06Rik	59	Lgmn	88	Rrm2b
2	2010001M09Rik	31	Ddc	60	Lgr5	89	Rsph1
3	Adrbk1	32	Dnajc7	61	LOC100047815	90	Sbk
4	Agpat9	33	Dok3	62	LOC637082	91	Sdc4
5	Agtr1a	34	Dpp4	63	LOC676420	92	Sertad4
6	Akap12	35	Dusp2	64	Lrmp	93	Sgk1
7	Alox12	36	Emp1	65	Lxn	94	Slamf7
8	Aof1	37	Ets1	66	Ly6d	95	Slc12a3
9	Apobec1	38	Fam169b	67	Marcks	96	Smarca4
10	Arhgap24	39	Fbxl12	68	Myl4	97	Smtnl2
11	Arl5c	40	Fcrla	69	Nedd9	98	Snap29
12	Arntl	41	Fgf13	70	Nfkbie	99	Snn
13	Arpc5l	42	Foxo1	71	Nuak1	100	Spib
14	Atp1b1	43	Foxp1	72	Pafah1b3	101	Srpk3
15	Axud1	44	Gas7	73	Pde2a	102	St6gal1
16	B3gnt5	45	H2-M3	74	Plekha2	103	Stambpl1
17	Bach2	46	H2-Ob	75	Polm	104	Tmem108
18	Bcl7a	47	Hdac5	76	Pou2af1	105	Tmem132e
19	Blk	48	Herpud1	77	Ppbp	106	Tmprss3
20	Blnk	49	Hmgn3	78	Ppm1e	107	Tnfrsf13c
21	Ccng2	50	Hspa2	79	Prep	108	Tnfrsf19
22	Cd19	51	Igf2bp3	80	Prkcb	109	Tpm4
23	Cd1d1	52	Il12a	81	Prm1	110	Trp53i11
24	Cd79b	53	Il16	82	Pscd1	111	Trp53inp1
25	Cdk5r1	54	Il7r	83	Ptp4a3	112	Ttpal
26	Chst3	55	Irf4	84	Ptprcap	113	Tubb2b
27	Cnp	56	Jakmip1	85	Rapgefl1	114	Uchl1
28	Coq7	57	Klhl6	86	Rasgrp1	115	Vpreb3
29	Csrp2	58	Lbh	87	Rpe	116	Zhx2

Table S2 – List of 116 genes in CD45- BM stromal cells that matched the pattern where they were increased in expression between untreated 9mo and untreated 2mo mice with mice that had been given SSA increasing their gene expression temporally after surgery.